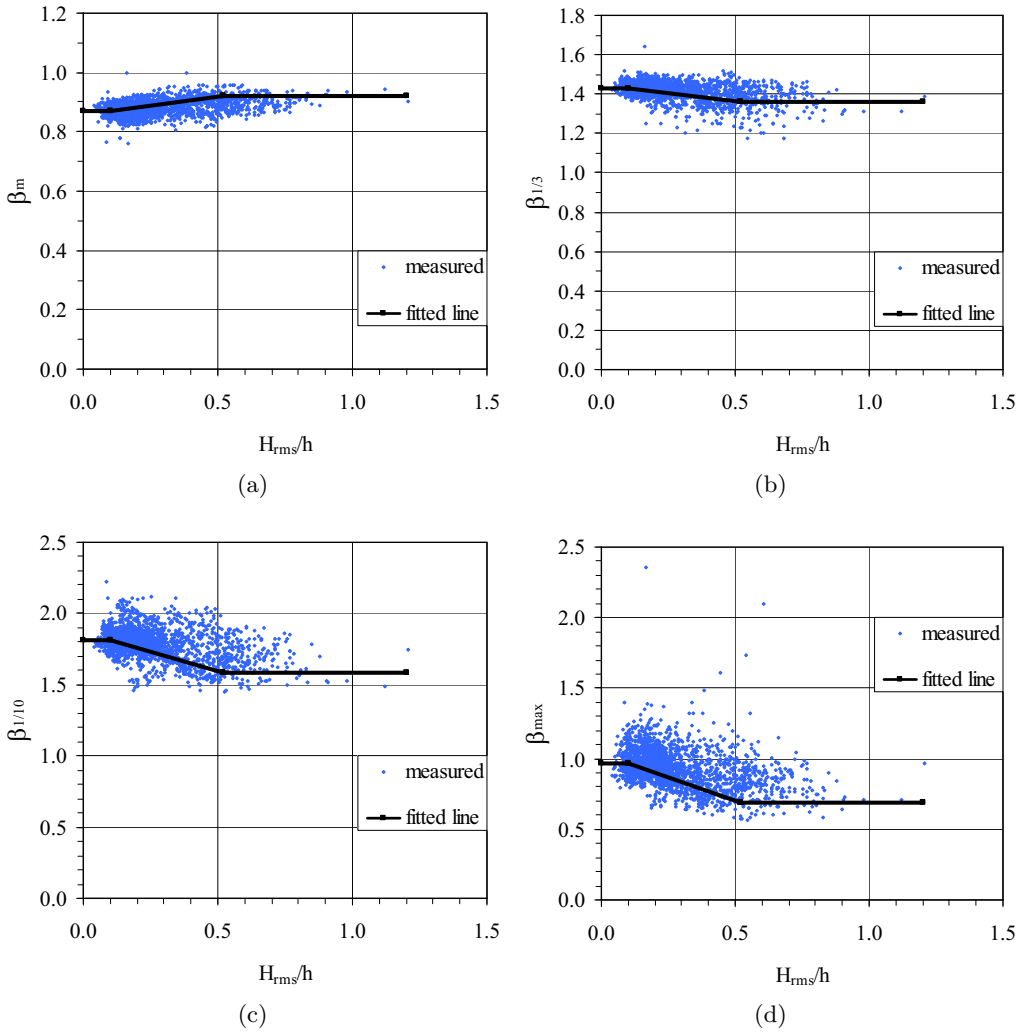

Fig. 1. Relationships between H_{rms}/h versus (a) β_m, (b) $\beta_{1/3}$, (c) $\beta_{1/10}$, and (d) $\beta_{\max}$.

relationships in Figs. 1 to 3, it is not clear which dimensionless parameter gives the best correlation. Therefore, all of them are considered to determine the coefficients β.

It can be seen from Figs. 1 to 3 that the relationships can be separated into 3 zones. The coefficients β are constant for the first zone then gradually changed in the second zone and finally become constant again in the third zone. These 3 zones seem to correspond with the zone in coastal region, especially for Fig. 3. The zone in coastal region may be separated into 3 zones based on the fraction of breaking waves (Q_b) as offshore zone ($Q_b = 0$), outer surf zone ($0 < Q_b < 1.0$), and inner surf zone ($Q_b = 1$). According to Eq. (15), $Q_b = 0$ when $H_{rms}/H_b \leq 0.43$ and $Q_b = 1$ when $H_{rms}/H_b \geq 1.0$. These criteria seem to correspond well with the zones in Fig. 3.

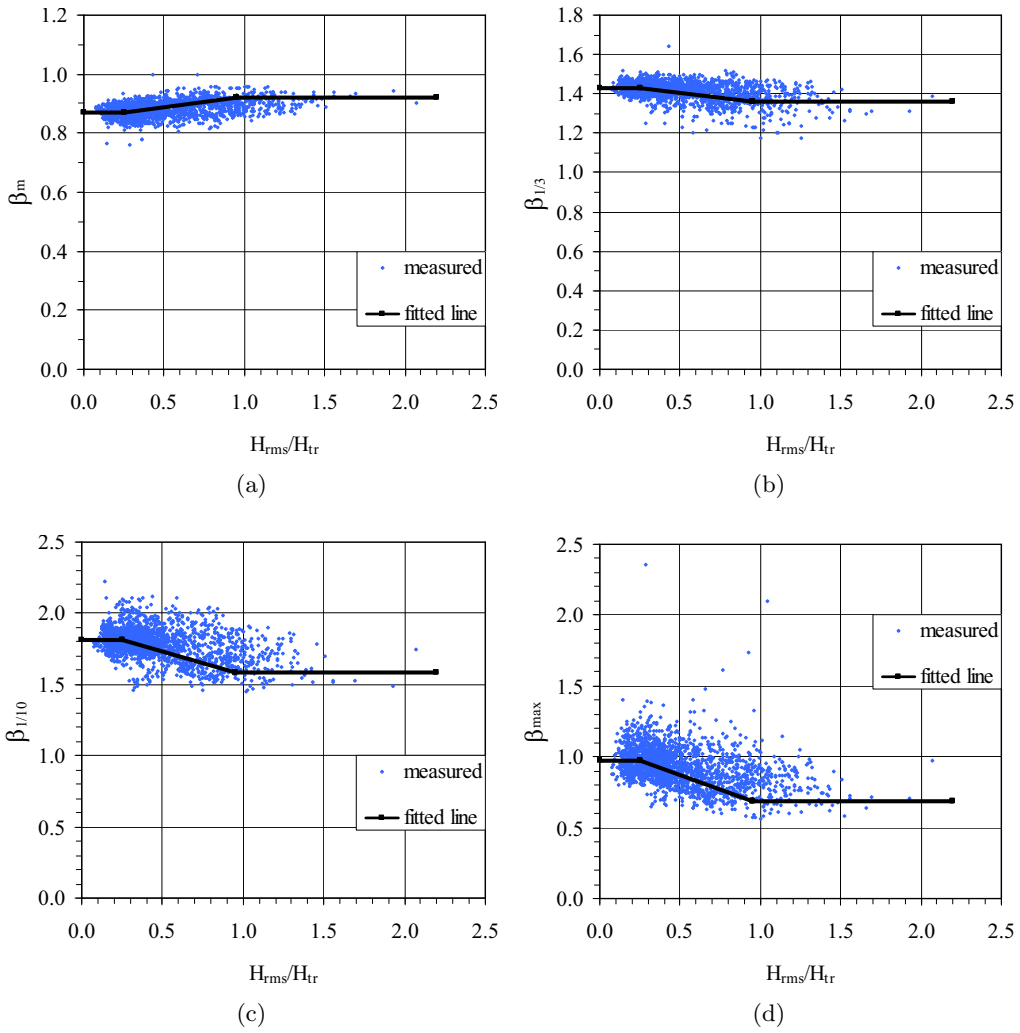

Fig. 2. Relationships between H_{rms}/H_{tr} versus (a) β_m, (b) $\beta_{1/3}$, (c) $\beta_{1/10}$, and (d) $\beta_{\max}$.

Thus, the 3 zones of coefficients β in Figs. 1 to 3 may be considered as offshore zone, outer surf zone, and inner surf zone. The coefficients β are constants for the offshore zone then gradually changed in the outer surf zone and finally become constants again in the inner zone. Therefore, the general form of β, which can be applied to β_m, $\beta_{1/3}$, $\beta_{1/10}$, and $\beta_{\max}$, is expressed as:

$$\beta = K_1 \qquad \text{for } X \le x_1 \tag{18a}$$

$$\beta = K_1 + \frac{(K_2 - K_1)}{(x_2 - x_1)}(X - x_1) \quad \text{for } x_1 < X < x_2 \tag{18b}$$

$$\beta = K_2 \qquad \text{for } X \ge x_2 \tag{18c}$$

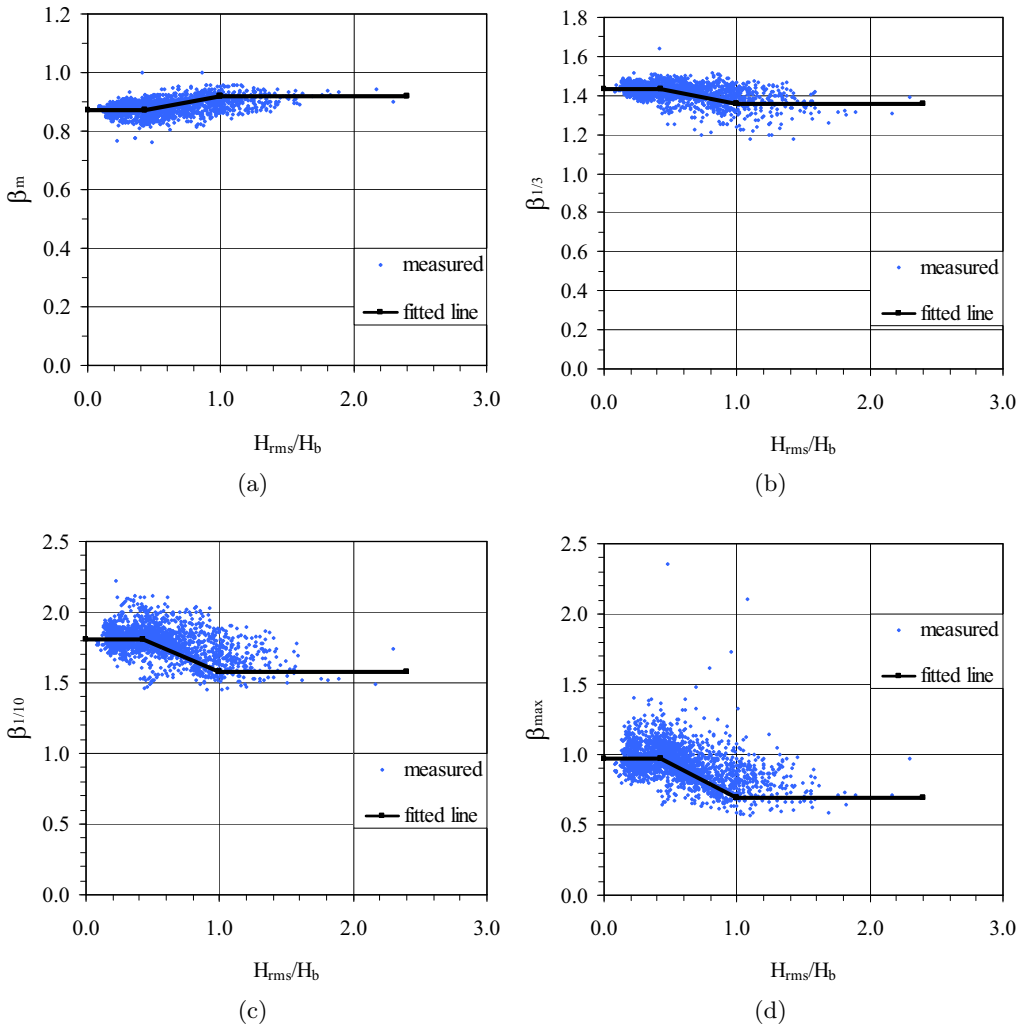

Fig. 3. Relationships between H_{rms}/H_b versus (a) β_m, (b) $\beta_{1/3}$, (c) $\beta_{1/10}$, and (d) $\beta_{\max}$.

where X is the dimensionless parameter (H_{rms}/h or H_{rms}/H_{tr} or H_{rms}/H_b), and K_1, K_2, x_1, and x_2 are constants which can be determined from formula calibration.

3.2. *Formula calibration*

The approximated values of the constants K_1, K_2, x_1, and x_2 for β_m, $\beta_{1/3}$, $\beta_{1/10}$ and $\beta_{\max}$ are determined from visual fit of Figs. 1 to 3. These approximated values are use as the initial values in the calibration. Using the coefficients β from Eq. (18) with the given constants (K_1, K_2, x_1, and x_2), the corresponding representative wave heights ($\bar{H}$, $H_{1/3}$, $H_{1/10}$, and $H_{\max}$) are computed from Eqs. (9) to (12), respectively. Then the errors (ER_g and ER_{avg}) for each representative wave height have been computed from Eqs. (7) and (8). The calibration of each formula is performed by

gradually adjusting the constants K_1, K_2, x_1, and x_2 until the error (ER_{avg}) becomes minimum. The general formulas of β (β_m, $\beta_{1/3}$, $\beta_{1/10}$ and $\beta_{\max}$) in terms of H_{rms}/h, H_{rms}/H_{tr}, and H_{rms}/H_b are expressed as follows:

(a) Formula of coefficients β in terms of H_{rms}/h:

$$\beta = K_1 \qquad \text{for } \frac{H_{rms}}{h} \leq 0.10 \tag{19a}$$

$$\beta = K_1 + \frac{(K_2 - K_1)}{(0.52 - 0.10)}\left(\frac{H_{rms}}{h} - 0.10\right) \quad \text{for } 0.10 < \frac{H_{rms}}{h} < 0.52 \tag{19b}$$

$$\beta = K_2 \qquad \text{for } \frac{H_{rms}}{h} \geq 0.52 \tag{19c}$$

(b) Formula of coefficients β in terms of H_{rms}/H_{tr}:

$$\beta = K_1 \qquad \text{for } \frac{H_{rms}}{H_{tr}} \leq 0.25 \tag{20a}$$

$$\beta = K_1 + \frac{(K_2 - K_1)}{(0.95 - 0.25)}\left(\frac{H_{rms}}{H_{tr}} - 0.25\right) \quad \text{for } 0.25 < \frac{H_{rms}}{H_{tr}} < 0.95 \tag{20b}$$

$$\beta = K_2 \qquad \text{for } \frac{H_{rms}}{H_{tr}} \geq 0.95 \tag{20c}$$

(c) Formula of coefficients β in terms of H_{rms}/H_b:

$$\beta = K_1 \qquad \text{for } \frac{H_{rms}}{H_b} \leq 0.43 \tag{21a}$$

$$\beta = K_1 + \frac{(K_2 - K_1)}{(1.0 - 0.43)}\left(\frac{H_{rms}}{H_b} - 0.43\right) \quad \text{for } 0.43 < \frac{H_{rms}}{H_b} < 1.0 \tag{21b}$$

$$\beta = K_2 \qquad \text{for } \frac{H_{rms}}{H_b} \geq 1.0 \tag{21c}$$

in which the best fitted constants (K_1 and K_2) for coefficients β_m, $\beta_{1/3}$, $\beta_{1/10}$, and $\beta_{\max}$ are shown in Table 4. The fitted lines from Eqs. (19) to (21) are shown as the solid lines in Figs. 1 to 3.

Table 4. Best fitted constants K_1 and K_2 for the coefficients β_m, $\beta_{1/3}$, $\beta_{1/10}$ and $\beta_{\max}$.

Constants	Coefficients β			
	β_m	$\beta_{1/3}$	$\beta_{1/10}$	$\beta_{\max}$
K_1	0.87	1.43	1.81	0.97
K_2	0.92	1.36	1.58	0.69

The examinations of Eqs. (19) to (21) are carried out by using the measured representative wave heights (i.e. H_{rms}, $\bar{H}$, $H_{1/3}$, $H_{1/10}$, and $H_{\max}$) from Table 1. The representative wave heights are computed by substituting the corresponding equation of coefficients β [from Eqs. (19) to (20)] into Eqs. (9) to (12). Table 5 shows the errors (ER_g and ER_{avg}) of Eqs. (19) to (21) on computing $\bar{H}$, $H_{1/3}$, $H_{1/10}$, and $H_{\max}$ for three groups of experiment scale while Table 6 shows the errors (ER_g) for all groups of major test. The results from Tables 5 and 6 are summarized as follows:

(a) Comparison among the overall errors (ER_{avg}) of Eqs. (19) to (21), Eq. (21) seems to be the best. This means that the variation of coefficients β is mainly governed by the fraction of breaking waves (or H_{rms}/H_b).
(b) Comparing with the relationships derived from Rayleigh distribution [Eqs. (3) to (5)], Eq. (21) gives slightly better estimation on $\bar{H}$, $H_{1/3}$, $H_{1/10}$ for large-scale and field experiments and give considerably better for small-scale experiments. For estimating $H_{\max}$, the accuracy of Eq. (21) is significantly better than that derived from Rayleigh distribution [Eq. (6)] for the three experiment-scales.
(c) The overall average errors (ER_{avg}) of Eq. (21) for computing $\bar{H}$, $H_{1/3}$, $H_{1/10}$, and $H_{\max}$ are 3.1%, 4.5%, 6.0%, and 12.2% respectively. In comparison with ER_{avg} of Eqs. (3) to (6) that shown in Table 2, Eq. (21) gives slightly better accuracy on the estimation of $\bar{H}$ and $H_{1/3}$, gives better accuracy on the estimation of $H_{1/10}$, and gives significantly better accuracy on the estimation of $H_{\max}$.

As Eq. (21) is better than the relationships derived from the Rayleigh distribution [Eqs. (3) to (6)], it may be used to indicate the limitation of Rayleigh distribution in shallow water. Equation (21) reveals some limitations of the Rayleigh distribution as follows:

(a) In the offshore zone ($H_{rms}/H_b \leq 0.43$), the coefficients β_m, $\beta_{1/3}$, $\beta_{1/10}$, and $\beta_{\max}$ are equal to 0.87, 1.43, 1.81, and 0.97 respectively. These values are nearly the same as those derived from the Rayleigh distribution. This shows that the Rayleigh distribution may be valid not only in the deepwater but also in the offshore zone or non-breaking wave zone. This also reveals the limitation of the present formulas. The formulas are limited to be used for the cases that the wave height distribution in the deepwater (or in the offshore zone) is close to the Rayleigh distribution. In the field, it has been shown by many researchers that the deepwater wave height distribution obeys the Rayleigh distribution. However, for cases of laboratory experiments, irregular wave behavior is dependent on the given wave history to wave generator. The present formula should be used only for cases that the incident wave height distribution is close to the Rayleigh distribution (e.g. JONSWAP and TMA spectrums).
(b) In the surf zones ($H_{rms}/H_b > 0.43$), the coefficients $\beta_{1/3}$, $\beta_{1/10}$, and $\beta_{\max}$ are smaller than those derived from the Rayleigh distribution. This shows that

Table 5. The errors (ER_g and ER_{avg}) of present formulas [Eqs. (19) to (21)] on the estimation of $\bar{H}$, $H_{1/3}$, $H_{1/10}$, and $H_{\max}$ for three groups of experiment scale.

Experiments	Eq. (19)				Eq. (20)				Eq. (21)			
	$\bar{H}$	$H_{1/3}$	$H_{1/10}$	$H_{\max}$	$\bar{H}$	$H_{1/3}$	$H_{1/10}$	$H_{\max}$	$\bar{H}$	$H_{1/3}$	$H_{1/10}$	$H_{\max}$
Small-scale	3.2	6.9	6.3	15.6	3.3	7.0	6.4	16.5	3.2	6.9	7.0	14.6
Large-scale	2.6	2.6	6.4	13.8	2.6	2.6	6.1	13.2	2.5	2.5	5.9	12.7
Field	3.9	3.1	5.2	9.1	4.3	3.5	6.2	11.4	3.7	2.8	4.9	8.5
ER_{avg}	3.3	4.6	6.0	13.1	3.5	4.8	6.2	13.9	3.1	4.5	6.0	12.2

Table 6. The errors (ER_g) of present formulas [Eq. (19) to (21)] on the estimation of $\bar{H}$, $H_{1/3}$, $H_{1/10}$, and $H_{\max}$ for all groups of major test.

Major test No.	Eq. (19)				Eq. (20)				Eq. (21)			
	$\bar{H}$	$H_{1/3}$	$H_{1/10}$	$H_{\max}$	$\bar{H}$	$H_{1/3}$	$H_{1/10}$	$H_{\max}$	$\bar{H}$	$H_{1/3}$	$H_{1/10}$	$H_{\max}$
SKR2	3.2	8.0	N.A.*	20.6	3.3	8.1	N.A.*	22.0	2.9	7.9	N.A.*	17.4
SKR6	3.4	7.8	N.A.*	14.8	3.5	7.9	N.A.*	15.5	3.4	7.7	N.A.*	14.4
SKR8	3.2	5.2	N.A.*	10.1	3.3	5.3	N.A.*	10.7	3.5	5.4	N.A.*	11.5
Ting1	1.6	3.4	5.2	12.2	1.6	3.4	5.4	12.3	1.9	3.5	5.9	12.9
Ting2	2.9	5.8	7.4	12.9	3.0	5.8	7.5	13.4	3.2	5.9	8.2	15.6
ST10	1.5	1.7	3.9	10.2	1.6	1.6	3.5	10.2	1.4	1.6	3.4	8.7
ST20	2.3	2.1	4.9	11.8	2.3	2.2	4.7	11.3	2.2	2.0	4.3	10.8
ST30	3.9	3.5	8.5	18.8	3.7	3.3	8.0	17.8	3.4	3.1	7.5	16.8
ST40	3.4	2.7	9.0	17.6	3.2	2.5	8.4	16.1	3.1	2.5	8.2	15.7
ST50	2.0	2.1	5.0	12.5	2.0	2.1	4.5	11.4	2.0	2.0	4.2	11.1
ST60	1.9	2.0	6.2	14.0	1.8	1.8	5.5	12.4	1.6	1.7	5.2	11.8
ST70	2.1	2.0	4.7	11.5	2.0	1.9	4.1	10.4	2.0	1.8	3.9	10.4
ST80	2.5	2.7	7.1	13.2	2.2	2.5	6.3	12.1	2.2	2.4	5.9	11.9
ST90	1.8	2.2	4.7	8.3	1.6	2.0	4.0	7.5	1.9	2.3	4.8	8.5
STAO	4.6	4.2	4.9	5.4	4.0	3.8	3.9	4.8	4.4	4.1	4.6	5.4
STCO	2.6	2.2	6.2	14.6	2.6	2.1	5.7	13.5	2.5	2.1	5.8	13.8
STDO	2.9	3.0	4.4	11.8	3.1	3.2	5.0	12.6	2.9	3.0	4.3	11.5
STJO	2.9	3.5	8.1	14.9	3.0	3.6	8.2	15.2	2.8	3.5	8.0	15.1
STKO	2.7	2.9	5.8	11.2	2.9	3.1	6.1	11.4	2.9	3.1	6.2	11.8
Audrey	3.6	2.5	4.0	8.2	4.0	2.9	5.2	10.5	3.4	2.3	3.6	7.4
Bertha	2.3	2.4	4.8	8.6	2.8	2.8	5.6	10.9	2.1	2.2	4.4	8.1
Ella	4.5	4.3	6.1	9.4	5.0	4.9	7.4	12.7	4.3	4.0	5.5	8.0
Esther	4.6	2.4	5.5	9.7	4.9	2.8	5.9	11.1	4.4	2.2	5.4	10.1

*N.A. = Not Available

the Rayleigh distribution tends to give an overestimation of the larger wave heights. Oppositely, the coefficient β_m is slightly larger than that derived from the Rayleigh distribution. This shows that the Rayleigh distribution tends to give an underestimation of the smaller wave heights. The overestimation of large wave heights and underestimation of small wave heights of the Rayleigh distribution in the surf zone was also reported by Battjes and Groenendijk [2000].

(c) The gradual change of coefficients β in the outer surf zone ($0.43 < H_{rms}/H_b < 1.0$) indicates that the wave height distribution is gradually deviated from the Rayleigh distribution and the deviation becomes maximum at the inner surf zone ($H_{rms}/H_b \geq 1.0$). As the coefficients β are governed by H_{rms}/H_b and the fraction of breaking waves (total number of braking waves per total number waves, Q_b) is also governed by H_{rms}/H_b, it may be concluded that the coefficients β are governed by Q_b. The deviation of coefficients β from those of Rayleigh distribution in the surf zone ($H_{rms}/H_b > 0.43$) reveals that the wave breaking (or Q_b) is the main factor to cause the wave height distribution (or β) deviate from that of Rayleigh. Seaward of the incipient wave breaking ($H_{rms}/H_b < 0.43$), the wave height distribution is close to the Rayleigh distribution as no wave is breaking ($Q_b = 0$). When the waves propagate onshore in the outer surf zone, the fraction of breaking waves (Q_b) increases as more and more waves are breaking. At each spatial point in the outer surf zone, there are both broken and unbroken waves. The broken wave heights decrease due to energy dissipation while the non-broken wave heights still increase due to wave shoaling. This causes the wave height distribution to deviate from the Rayleigh distribution. The deviation is gradually increased (as more and more waves are breaking) until almost all waves are breaking in the inner surf zone.

It should be noted that Eq. (21) is an empirical formula. Its validity may be limited according to the range of experimental conditions that are employed in the calibration. The present formula should be applicable for deepwater wave steepness (H_{rmso}/L_o) ranging between 0.001 and 0.059 and it is limited to be used for cases that the wave height distribution in the deepwater (or in the offshore zone) is close to the Rayleigh distribution.

4. Conclusions

This study concentrates on the relationships for conversion from H_{rms} to be $\bar{H}$, $H_{1/3}$, $H_{1/10}$, and $H_{\max}$ for shallow water region. Widely accepted relationships are derived based on the assumption of the Rayleigh distribution. It is well known that the wave height distribution in shallow water deviates from the Rayleigh distribution. However, it is not clear whether this deviation can lead to significant errors on the estimation of representative wave heights or not. The first objective of this study is to investigate the errors of estimating representative wave heights by using the relationships derived from the Rayleigh distribution in shallow water.

Experimental data from small-scale, large-scale, and field experiments were used to examine the accuracy of the relationships. The examination showed that the assumption of Rayleigh distribution is not violated largely in shallow water, especially for large-scale and field experiments. The relationships derived from Rayleigh distribution give very good estimations on $\bar{H}$ and $H_{1/3}$, good estimation on $H_{1/10}$ but fair estimations on $H_{\max}$. The errors of small-scale experiments are considerably larger than those of large-scale and field experiments.

An attempt was made to improve the accuracy of the estimations. The proportional coefficients (β) in the relationships were plotted with three dimensionless parameters (H_{rms}/h, H_{rms}/H_{tr}, and H_{rms}/H_b). It was found that the coefficients β are governed mainly by the fraction of breaking waves (or H_{rms}/H_b) and the new coefficients β have been proposed as a function of H_{rms}/H_b. Comparing with the coefficients β derived from the Rayleigh distribution, the new coefficients β give slightly better accuracy on estimating $\bar{H}$ and $H_{1/3}$, and give better accuracy on estimating $H_{1/10}$ and $H_{\max}$. The new coefficients reveal that the Rayleigh distribution is valid in the offshore zone but gives overestimation of the number of large waves and underestimation of the number of small waves in the surf zone. The wave height distribution is gradually deviated from the Rayleigh distribution in the outer surf zone and the deviation becomes maximum at the inner surf zone.

Acknowledgments

This research was sponsored by the Thailand Research Fund.

References

Battjes, J. A. & Groenendijk, H. W. [2000] "Wave height distributions on shallow foreshores," *Coastal Engineering* **40**, 161–182.

Battjes, J. A. & Janssen, J. P. F. M. [1978] "Energy loss and set-up due to breaking of random waves," in *Proc. 16th Coastal Engineering Conf. ASCE*, pp. 569–589.

Dally, W. R. [1990] "Random breaking waves: A closed-form solution for planar beaches," *Coastal Engineering* **14**, 233–263.

Dean, R. G. & Dalrymple, R. A. [1994] *Water Wave Mechanics for Engineers and Scientists* (World Scientific Publishing Co. Pte. Ltd.), p. 193.

Demerbilek, Z. & Vincent, L. [2006] "Water wave mechanics (Part 2 — Chapter 1)," Coastal Engineering Manual, EM1110-2-1100, Coastal and Hydraulics Laboratory — Engineering Research and Development Center, WES, U.S. Army Corps of Engineers, pp. II-1-75.

Elfrink, B., Hanes, D. M. & Ruessink, B. G. [2006] "Parameterization and simulation of near bed orbital velocities under irregular waves in shallow water," *Coastal Engineering* **53**, 915–927.

Goda, Y. [1970] "A synthesis of breaking indices," *Transaction Japan Society of Civil Engineers* **2**, 227–230.

Goda, Y. [1974] "Estimation of wave statistics from spectral information," in *Proc. Ocean Waves Measurement and Analysis Conference, ASCE*, pp. 320–337.

Goda, Y. [1977] "Numerical experiments on the statistical variability of ocean waves," *Rep. Port and Habour Research Institute* **16**, 3–26.

Goda, Y. [2000] *Random Seas and the Design of Maritime Structures* (World Scientific Publishing Co. Pte. Ltd.), p. 263.

Goodknight, R. C. & Russel, T. L. [1963] "Investigation of the statistics of wave heights," *J. Waterways and Harbors Division, ASCE* **89**(WW2), 29–55.

Hughes, S. A. & Borgman, L. E. [1987] "Beta-Rayleigh distribution for shallow water wave heights," in *Proc. of the American Society of Civil Engineers Specialty Conference on Coastal Hydrodynamics*, ASCE, pp. 17–31.

Kraus, N. C. & Smith, J. M. [1994] SUPERTANK Laboratory Data Collection Project, Technical Report CERC-94-3, WES, U.S. Army Corps of Engineers, pp. 55–73.

Larson, M. [1995] "Model for decay of random waves in surf zone," *J. Waterway, Port, Coastal, and Ocean Engineering, ASCE* **121**(1), 1–12.

Longuet-Higgins, M. S. [1952] "On the statistical distribution of the heights of sea waves," *J. Marine Research* **11**(3), 245–266.

Mendez, F. J., Losada, I. J. & Medina, R. [2004] "Transformation model of wave height distribution on planar beaches," *Coastal Engineering* **50**, 97–115.

Rattanapitikon, W. & Shibayama, T. [1998] "Energy dissipation model for regular and irregular breaking waves," *Coastal Engineering Journal, JSCE* **40**(4), 327–346.

Rattanapitikon, W., Karunchintadit, R. & Shibayama, T. [2003] "Irregular wave height transformation using representative wave approach," *Coastal Engineering Journal, JSCE* **45**(3), 489–510.

Smith, J. M. & Kraus, N. C. [1990] Laboratory Study on Macro-Features of Wave Breaking over Bars and Artificial Reefs, Technical Report CERC-90-12, WES, U.S. Army Corps of Engineers, pp. 59–74 and C36-C39.

Thornton, E. B. & Guza, R. T. [1983] "Transformation of wave height distribution," *J. Geophysical Research* **88**(C10), 5925–5938.

Ting, F. C. K. [2001] "Laboratory study of wave and turbulence velocity in broad-banded irregular wave surf zone," *Coastal Engineering* **43**, 183–208.

Ting, F. C. K. [2002] "Laboratory study of wave and turbulence characteristics in narrow-banded irregular breaking waves," *Coastal Engineering* **46**, 291–313.

Ocean Engineering 35 (2008) 1259–1270

Contents lists available at ScienceDirect

Ocean Engineering

journal homepage: www.elsevier.com/locate/oceaneng

Verification of significant wave representation method

Winyu Rattanapitikon *

Civil Engineering Program, Sirindhorn International Institute of Technology, Thammasat University, Pathum Thani 12121, Thailand

ARTICLE INFO

Article history:
Received 14 August 2007
Accepted 18 March 2008
Available online 26 March 2008

Keywords:
Irregular wave model
Significant wave height
Representative wave approach
Significant wave representation method
Energy dissipation

ABSTRACT

The significant wave representation method is the simplest method for computing the transformation of significant wave height across-shore. However, many engineers are reluctant to use this method because many researchers have pointed out that the method possibly contains a large estimation error. Nevertheless, Rattanapitikon et al. [Rattanapitikon, W., Karunchintadit, R., Shibayama, T., 2003. Irregular wave height transformation using representative wave approach. Coastal Engineering Journal, JSCE 45(3), 489–510.] showed that the wave representation method could be used to compute the transformation of root mean square wave heights. It may also be possible to use it for computing the significant wave height transformation. Therefore, this study was carried out to examine the possibility of simulating significant wave height transformation across-shore by using the significant wave representation method. Laboratory data from small- and large-scale wave flumes were used to calibrate and examine the models. Six regular wave models were applied directly to irregular waves by using the significant wave height and spectral peak period. The examination showed that three regular wave models (with new coefficients) could be used to compute the significant wave height transformation with very good accuracy. On the strength of both accuracy and simplicity of the three models, a suitable model is recommended for computing the significant wave height transformation. The suitable model was also modified for better predictions. The modified model (with different coefficients) can be used to compute either regular wave height or significant wave height transformation across-shore.

1. Introduction

The significant wave height (which is defined as the average of the highest one-third wave heights) is most frequently used in the field of coastal and ocean engineering (Goda, 2000; Andreas and Wang, 2007), especially in the design of coastal and ocean structures. The wave heights are usually available in deepwater but not available at the required depths in shallow water. The wave heights in shallow water can be determined from wave models. Common approaches to model the significant wave height transformation may be classified into three main approaches, i.e., representative wave approach (commonly referred to as significant wave representation method), wave-by-wave approach, and conversion approach.

For the significant wave representation method, the regular wave models are directly applied to irregular waves by using the significant wave height. The method has been widely used since the introduction of the significant waves. It is easy to understand and also simple to use. However, the characteristics of the irregular waves (e.g., wave height and period) are statistically variable in contrast to regular waves, which have a single height, period, and direction. As the significant wave representation method does not consider such variability, the method may possibly contain a large estimation error (Goda, 2000).

The wave-by-wave approach considers the propagation of individual waves in the irregular wave train. The incident individual waves may be determined from irregular wave records or from probability density function (pdf) of wave heights. The propagation of each individual wave is computed by using an appropriate regular wave model. Recombining the individual wave heights at the required depth yields the irregular wave train, which is used to determine the significant wave height or other representative wave heights. Several models have been proposed based on this approach, differing mainly in the regular wave model used to simulate the propagation of the individual waves (e.g., the models of Mizuguchi, 1982; Dally, 1992; Kuriyama, 1996; Goda, 2004). This approach is particularly useful if a detailed wave height distribution is required. However, it has the disadvantage of being time consuming, which may not be suitable for some practical work.

The conversion approach is used to convert the representative wave heights from one to another through the known relationships. The root mean square wave height (H_{rms}) is usually used as a reference wave height of the conversion because it is the output

* Tel.: +66 2564 3221; fax: +66 2986 9112.
E-mail address: winyu@siit.tu.ac.th

0029-8018/$ - see front matter © 2008 Elsevier Ltd. All rights reserved.
doi:10.1016/j.oceaneng.2008.03.008

of many wave models (e.g., the models of Battjes and Janssen, 1978; Thornton and Guza, 1983; Larson, 1995; Rattanapitikon, 2007). Therefore, the significant wave height (H_s) can be determined from the known relationship between H_{rms} and H_s (e.g., the relationships of Longuet-Higgins, 1952; Battjes and Groenendijk, 2000; Rattanapitikon and Shibayama, 2007). This approach is simpler than the wave-by-wave approach but slightly more complicated than the significant wave representation method.

The present study focuses on the significant wave representation method, as this appears to be the simplest method. Many researchers pointed out that the significant wave representation method could give inconsistent or erroneous results in the computation of significant wave height transformation (Goda, 2000). It seems that no literature has pointed out that the significant wave representation method is applicable in the surf zone. Consequently, engineers have been reluctant to use the significant wave representation method. However, the significant wave representation method has the merits of easy understanding, simple application and it is not necessary to assume the shape of the pdf of wave heights. It will be useful for some practical work if this approach can be used to compute the significant wave heights in shallow water. Moreover, Rattanapitikon et al. (2003) reported that the representative wave approach can be used to compute H_{rms} with very good accuracy. It may also be used to compute H_s. This study is carried out to investigate the possibility of using the significant wave representation method.

This paper is divided into four main parts. The first part describes the collected data. The second part describes some existing regular wave models. The third part describes modeling of irregular waves using significant wave representation method. The fourth part deals with the modification of the selected model.

2. Collected laboratory data

For the significant wave representation method, the regular wave model is directly applied to irregular waves by using the significant wave height. The present study is, therefore, concerned with both regular and irregular wave models. The experiments performed under regular and irregular wave conditions are used to calibrate and examine the models.

2.1. Regular wave data

Laboratory data of regular wave heights inside the surf zone from 13 sources (total 492 cases) have been collected for calibration and examination of the regular wave models. The experiments cover a wide range of wave and bottom topography conditions, including small- and large-scale experiments. The experiments cover a variety of beach conditions and cover a range of deepwater wave steepness (H_o/L_o, where H_o is the deepwater wave height and L_o is the deepwater wavelength) from 0.003 to 0.112. A summary of the collected laboratory data is given in Table 1. Most of the experiments were carried out in small-scale wave flumes, except the experiments of Kajima et al. (1983) and Kraus and Smith (1994) which were carried out in large-scale wave flumes. The data sources are the same as those used by Rattanapitikon et al. (2003).

2.2. Irregular wave data

Laboratory data of significant wave height transformation from six sources, totaling 282 cases, were collected for calibration and examination of the irregular wave models. A summary of the collected laboratory data is shown in Table 2. The collected data are separated into two groups based on the experiment-scale, i.e., small- and large-scale experiments. The experiments of Hurue (1990), Smith and Kraus (1990), Katayama (1991), and Ting (2001) were performed in small-scale wave flumes under fixed bed conditions, while the experiments of Kraus and Smith (1994) and Dette et al. (1998) were undertaken in large-scale wave flumes under movable bed (sandy bed) conditions. The data cover a range of deepwater wave steepness (H_{so}/L_o, where H_{so} is the deepwater significant wave height) from 0.002 to 0.064. A brief description of the experiments is given below.

The experiment of Hurue (1990) was conducted to study wave and undertow velocity on a plane beach. The experiment was performed in a small-scale wave flume, which was 17 m long and 0.5 m wide. The beach topography was 1/20 uniform slope with the smooth bottom. The incident significant wave height of 0.09 m and wave period of 1.26 s was generated based on the Bretschneider–Mitsuyasu spectrum (Bretschneider, 1968; Mitsuyasu, 1970). Water surface elevations were measured at seven cross-shore locations using a capacitance-type gage.

The experiment of Smith and Kraus (1990) was conducted to investigate the macro-features of wave breaking over bars and artificial reefs using a small wave flume of 45.70 m long, 0.46 m wide, and 0.91 m deep. Both regular and irregular waves were employed in this experiment. A total of 12 cases were performed for irregular wave tests. Three irregular wave conditions were generated for three bar configurations as well as for a plane beach. A JONSWAP (Hasselmann et al., 1973) computer signal was generated for spectral width parameter of 3.3 and spectral peak periods of 1.07, 1.56, and 1.75 s with significant wave heights of

Table 1
Summary of collected experimental data used to calibrate and verify the regular wave models

Sources	Beach condition	No. of cases	No. of data	H_o/L_o
Cox and Kobayashi (1997)	Plane beach	1	5	0.015
Hansen and Svendsen (1984)	Plane beach	1	5	0.019
Horikawa and Kuo (1966)	Plane and stepped beach	213	2127	0.006–0.100
Hurue (1990)	Plane beach	1	4	0.038
Nadaoka et al. (1982)	Plane beach	2	11	0.013–0.080
Nagayama (1983)	Plane, stepped, and barred beach	12	171	0.025–0.055
Okayasu et al. (1988)	Plane beach	10	62	0.009–0.054
Sato et al. (1988)	Plane beach	3	25	0.031–0.050
Sato et al. (1989)	Plane beach	2	11	0.019–0.036
Shibayama and Horikawa (1985)	Sandy beach	10	85	0.028–0.036
Smith and Kraus (1990)	Plane and barred beach	101	506	0.008–0.096
Kajima et al. (1983)	Sandy beach	79	1397	0.003–0.112
Kraus and Smith (1994)	Sandy beach	57	429	0.003–0.066
Total		492	4838	0.003–0.112

Table 2
Summary of collected experimental data used to calibrate and verify the irregular wave models

Sources	Test series	Descriptions	No. of cases	No. of data	H_{so}/L_o
Hurue (1990)	Hu1	Plane beach	1	7	0.037
Smith and Kraus (1990)	R2000	Plane beach	1	8	0.070
	R22xx	Barred beach	3	24	0.070
	R6000	Plane beach	1	8	0.040
	R62xx	Barred beach	3	24	0.040
	R8000	Plane beach	1	8	0.030
	R82xx	Barred beach	3	24	0.030
Katayama (1991)	Ka1&Ka2	Barred beach	2	16	0.041, 0.044
Ting (2001)	Ti1	Plane beach	1	7	0.024
Kraus and Smith (1994)	ST10	Erosion toward equilibrium	26	416	0.013–0.064
	ST20	Acoustic profiler tests	8	128	0.002–0.057
	ST30	Accretion toward equilibrium	19	304	0.003–0.007
	ST40	Dedicated hydrodynamics	12	192	0.005–0.050
	ST50	Dune erosion, test 1	8	128	0.012–0.057
	ST60	Dune erosion, test 2	9	144	0.009–0.022
	ST70	Seawall, test 1	9	144	0.022–0.032
	ST80	Seawall, test 2	3	48	0.022
	ST90	Berm flooding, test 1	3	48	0.050
	STAO	Foredune erosion	1	16	0.050
	STCO	Seawall, test 3	8	127	0.004–0.057
	STDO	Berm flooding, test 2	3	48	0.050
	STJO	Narrow-crested mound	10	160	0.005–0.050
	STKO	Broad-crested mound	9	144	0.005–0.050
Dette et al. (1998)	A8	1:20 beach slope, normal	7	147	0.010
	A9	1:20 beach slope, storm	15	390	0.018
	B1	1:10 beach slope, normal	8	191	0.010
	B2	1:10 beach slope, storm	15	392	0.018
	C1	1:5 beach slope, normal	4	95	0.010
	C2	1:5 beach slope, storm	17	459	0.018
	H1	1:15 beach slope, normal	2	43	0.010
	H2	1:15 beach slope, storm	15	398	0.018
	D1&D3	D.P.[a], no overtopping, normal	7	158	0.010
	D2	D.P.[a], no overtopping, storm	11	297	0.018
	E	D.P.[a], with overtopping, storm	11	297	0.018
	F	No D.P.[a], storm	12	324	0.018
	G	No D.P.[a], underwater barrier	14	365	0.012–0.018
Total			282	5729	0.002–0.064

[a] D.P., dune protection.

0.12, 0.15, and 0.14 m, respectively. Water surface elevations were measured at eight cross-shore locations using resistance-type gages.

The experiment of Katayama (1991) was conducted to study wave and undertow velocity on a bar-type beach. The experiment was performed in a small-scale wave flume, which was 17 m long and 0.5 m wide. The bar-type beach consisted of the first 5 m of 1/20, the next 1 m of −1/20, and the last 4 m of 1/20 slopes. The incident significant wave heights of 0.06 and 0.08 m and wave periods of 0.95 and 1.14 s were generated based on the Bretschneider–Mitsuyasu spectrum (Bretschneider, 1968; Mitsuyasu, 1970). Water surface elevations were measured at eight cross-shore locations using a capacitance-type gages.

The experiment of Ting (2001) was conducted to study wave and turbulence velocities in a broad-banded irregular wave surf zone. The experiment was performed in a small-scale wave flume, which was 37 m long, 0.91 m wide, and 1.22 m deep. A false bottom with 1/35 slope built of marine plywood was installed in the flume to create a plane beach. The irregular waves were developed from the TMA spectrum (Bouws et al., 1985), with a spectral peak period of 2.0 s, a spectrally based significant wave height of 0.15 m and spectral width parameter of 3.3. Water surface elevations were measured at seven cross-shore locations using a resistance-type gage.

The SUPERTANK laboratory data collection project (Kraus and Smith, 1994) was conducted to investigate cross-shore hydrodynamic and sediment transport processes from August 5 to September 13, 1992 at Oregon State University, Corvallis, OR, USA. A 76-m-long sandy beach was constructed in a large wave tank of 104 m long, 3.7 m wide, and 4.6 m deep. Wave conditions included both regular and irregular waves. In all, 20 major tests were performed, and each major test consisted of several cases. Most of the tests (14 major tests) were performed under the irregular wave actions. The wave conditions were designed to balance the need for repetition of wave conditions to move the beach profile toward equilibrium and development of a variety of conditions for hydrodynamic studies. The TMA spectral shape (Bouws et al., 1985) was used to design all irregular wave tests. The collected experiments for irregular waves included 128 cases of wave and beach conditions (a total of 2047 wave records), covering incident significant wave heights from 0.2 to 1.0 m, spectral peak periods from 3.0 to 10.0 s, and spectral width parameter between 3.3 (broad-banded) and 100 (narrow-banded). Sixteen resistance-type gages were used to measure water surface elevations across-shore.

SAFE Project (Dette et al., 1998) was carried out to improve the methods of design and performance assessment of beach nourishment. The SAFE Project consisted of four activities, one of

which was to perform experiments in a large-scale wave flume in Hannover, Germany. A 250-m-long sandy beach was constructed in a large wave tank of 300 m long, 5 m wide, and 7 m deep. The test program was divided into two major phases. The first phase (cases A, B, C, and H) was aimed to study the beach deformation of equilibrium profile with different beach slope changes. The equilibrium beach profile was adopted from Bruun's (1954) approach ($h = 0.12x^{2/3}$). In the second phase, the sediment transport behaviors of dunes with and without structural aid were investigated (cases D, E, F, and G). The TMA spectral shape (Bouws et al., 1985) was used to design all irregular wave tests. The tests were performed under normal wave conditions ($H_{so}/L_o = 0.010$, water depth in the horizontal section = 4.0 m) and storm wave conditions ($H_{so}/L_o = 0.018$, water depth in the horizontal section = 5.0 m). A total of 27 wave gages was installed over a length of 175 m along one wall of the flume. The collected experiments included 138 cases of wave and beach conditions, covering deepwater wave steepness (H_{so}/L_o) from 0.010 to 0.018.

3. Regular wave model

The regular wave height transformation across-shore can be computed from the energy flux conservation as

$$\frac{\partial(Ec_g)}{\partial x} = -D_B, \tag{1}$$

where $E = \rho g H^2/8$ is the wave energy density, ρ is the water density, g is the acceleration due to gravity, H is the wave height, c_g is the group velocity, x is the distance in cross-shore direction, and D_B is the energy dissipation rate due to wave breaking which is zero outside the surf zone. The energy dissipation rate due to bottom friction is neglected. In the present study, all variables are based on the linear wave theory.

The wave height transformation can be computed from the energy flux conservation (Eq. (1)) by substituting the formula of the energy dissipation rate (D_B) and numerically integrating from offshore to shoreline. The difficulty of Eq. (1) is how to formulate the energy dissipation rate caused by the breaking waves.

During the past decades, various models have been developed for computing the energy dissipation of regular wave breaking. Widely used concepts for computing energy dissipation rate (D_B) for regular wave breaking are the bore concept and the stable energy concept.

The bore concept is based on the similarity between the breaking wave and the hydraulic jump. Several models have been proposed based on slightly different assumptions on the conversion from energy dissipation of hydraulic jump to energy dissipation of a breaking wave. Some existing D_B models, which were developed based on the bore concept, are listed as follows:

(a) Battjes and Janssen (1978):

$$D_B = 0.47\frac{\rho g H^2}{4T}, \tag{2}$$

(b) Thornton and Guza (1983):

$$D_B = 0.67\frac{\rho g H^3}{4Th}, \tag{3}$$

(c) Deigaard et al. (1991):

$$D_B = 0.48\frac{\rho g h H^3}{T(4h^2 - H^2)}, \tag{4}$$

where h is the water depth and T is the wave period. The constants in the above models were calibrated by Rattanapitikon et al. (2003) based on a wide range of experimental conditions as shown in Table 1.

The stable energy concept was introduced by Dally et al. (1985) based on an analysis of the measured breaking wave height on horizontal slope of Horikawa and Kuo (1966). When a breaking wave enters an area with horizontal bed, the breaking continues (the wave height decreases) until some stable wave height is attained. The development of the stable energy concept was based on an observation of stable wave height on horizontal slope. Dally et al. (1985) assumed that the energy dissipation rate was proportional to the difference between the local energy flux per unit depth and the stable energy flux per unit depth. Several models have been proposed on the basis of this concept. The main difference is the formula for computing the stable wave height (for more detail, please see Rattanapitikon et al., 2003). Some existing D_B models, which were developed based on the stable energy concept, are listed as follows:

(a) Dally et al. (1985):

$$D_B = 0.15\frac{\rho g c_g}{8h}[H^2 - (0.4h)^2], \tag{5}$$

(b) Rattanapitikon and Shibayama (1998):

$$D_B = 0.15\frac{\rho g c}{8h}\left\{H^2 - \left[h\exp\left(-0.36 - \frac{1.25h}{\sqrt{LH}}\right)\right]^2\right\}, \tag{6}$$

(c) Rattanapitikon et al. (2003):

$$D_B = 0.15\frac{\rho g c_g}{8h}\{H^2 - [0.073L\tanh(kh)]^2\}, \tag{7}$$

where c is the local phase velocity, L is the local wavelength, and k is the local wave number. The second terms on the right-hand side of Eqs. (5)–(7) are the terms of stable wave height. The energy dissipation will be zero if the wave height is less than the stable wave height.

The verification results of the six existing models are presented in the paper by Rattanapitikon et al. (2003). The results are also shown in Table 6 for comparison with the modified model (described in Section 5).

4. Irregular wave model

For the representative wave approach, the energy flux of the representative wave represents the average energy flux of an irregular wave train. The governing equation (energy flux conservation) of the representative wave (H_{rms}) can be derived based on the assumptions of linear wave theory and Rayleigh distribution of wave heights. Although the crude assumptions of the representative wave approach may not be theoretically justified (mainly because of the non-linearity of each individual wave), the approach is physically valid (the prediction agrees well with actual measurements). There are many wave models that are successful in using the energy flux conservation of the representative wave (H_{rms}) for computing the transformation of H_{rms} across-shore, e.g., the models of Battjes and Janssen (1978), Thornton and Guza (1983), Larson (1995), Baldock et al. (1998), Ruessink et al. (2003), and Rattanapitikon (2007). If the energy flux conservation of H_{rms} is valid, the energy flux conservation of H_s should also be valid because H_{rms} can be converted to H_s through the known coefficient (i.e., $H_s = 1.42H_{rms}$ for the Rayleigh

distribution). The derivation of the governing equation of the significant wave representation method is shown in the Appendix.

In the present study, for the significant wave representation method, the regular wave model is applied directly to irregular waves by using the significant wave height (H_s) and the spectral peak period (T_p). The spectral peak period is used because it is the most commonly used parameter and typically reported for the irregular wave data.

Since the D_B formulas shown in Section 3 (Eqs. (2)–(7)) were developed for regular waves, it is not clear which formula is suitable for the significant wave representation method. Therefore, all of them were used to investigate the possibility of simulating the significant wave height transformation.

Substituting the dissipation formula (Eqs. (2)–(7), respectively) into Eq. (1) and applying for significant wave height (H_s) and spectral peak period (T_p), the irregular wave models can be expressed as

$$\text{model (1)}: \quad \frac{\rho g}{8}\frac{\partial(H_s^2 c_g)}{\partial x} = -K_1 \frac{\rho g H_s^2}{4T_p}, \tag{8}$$

$$\text{model (2)}: \quad \frac{\rho g}{8}\frac{\partial(H_s^2 c_g)}{\partial x} = -K_2 \frac{\rho g H_s^3}{4T_p h}, \tag{9}$$

$$\text{model (3)}: \quad \frac{\rho g}{8}\frac{\partial(H_s^2 c_g)}{\partial x} = -K_3 \frac{\rho g h H_s^3}{T_p(4h^2 - H_s^2)}, \tag{10}$$

$$\text{model (4)}: \quad \frac{\rho g}{8}\frac{\partial(H_s^2 c_g)}{\partial x} = -K_4 \frac{\rho g c_g}{8h}[H_s^2 - (K_5 h)^2], \tag{11}$$

$$\text{model (5)}: \quad \frac{\rho g}{8}\frac{\partial(H_s^2 c_g)}{\partial x} = -K_6 \frac{\rho g c}{8h} \times \left\{H_s^2 - \left[K_7 h \exp\left(-0.36 - \frac{1.25h}{\sqrt{LH_s}}\right)\right]^2\right\}, \tag{12}$$

$$\text{model (6)}: \quad \frac{\rho g}{8}\frac{\partial(H_s^2 c_g)}{\partial x} = -K_8 \frac{\rho g c_g}{8h}\{H_s^2 - [K_9 L \tanh(kh)]^2\}, \tag{13}$$

where K_1–K_9 are the coefficients. It can be seen from Eqs. (2)–(7) that the coefficients K_1–K_9 for the regular wave models are 0.47, 0.67, 0.48, 0.15, 0.4, 0.15, 1.0, 0.15, and 0.073, respectively. When applying to the irregular wave, K_1–K_9 are the adjustable coefficients to allow for the effect of the transformation to irregular waves. Hereafter, Eqs. (8)–(13) are referred to as MD1, MD2, MD3, MD4, MD5, and MD6, respectively. The variables c_g, c, L, and k in the models MD1–MD6 are calculated based on the spectral peak period (T_p).

The breaking criterion of Miche (1944) (see also Tucker and Pitt, 2001, p. 307) is applied to determine incipient wave breaking of the significant wave height (H_{sb}) as

$$H_{sb} = K_{10} L \tanh(kh), \tag{14}$$

where K_{10} is the coefficient. The published value of K_{10} for regular wave breaking is 0.142. When applying to the irregular waves, K_{10} is the adjustable coefficient to allow for effect of the transformation to irregular waves. The energy dissipation (D_B) terms on the right-hand side of models MD1–MD6 occur when $H_s \geqslant H_{sb}$ and is equal to zero when $H_s < H_{sb}$.

4.1. Trial simulation

The objective of this section is to test the applicability of models MD1–MD6 by using the coefficients K_1–K_{10} which were proposed by the previous researchers for regular waves (shown in the second column of Table 3). All collected data shown in Table 2 are used to examine the models.

Table 3
The errors (ER_g and ER_{avg}) of the models MD1– MD6 (using the coefficients of regular waves) for two groups of experiment-scales (measured data from Table 2)

Models	Coefficients	ER_g		ER_{avg}
		Small-scale	Large-scale	
MD1 (Eq. (9))	$K_1 = 0.47$, $K_{10} = 0.142$	25.5	13.1	19.3
MD2 (Eq. (10))	$K_2 = 0.67$, $K_{10} = 0.142$	24.0	10.9	17.4
MD3 (Eq. (11))	$K_3 = 0.48$, $K_{10} = 0.142$	22.7	11.3	17.0
MD4 (Eq. (12))	$K_4 = 0.15$, $K_5 = 0.4$, $K_{10} = 0.142$	27.9	10.7	19.3
MD5 (Eq. (13))	$K_6 = 0.15$, $K_7 = 1.0$, $K_{10} = 0.142$	25.4	10.3	17.9
MD6 (Eq. (14))	$K_8 = 0.15$, $K_9 = 0.073$, $K_{10} = 0.142$	26.1	10.5	18.3

The basic parameter for determination of the overall accuracy of the model is the average rms relative error (ER_{avg}), which is defined as

$$ER_{avg} = \frac{\sum_{n=1}^{tn} ER_{gn}}{tn}, \tag{15}$$

where n is the data group number, ER_{gn} is the rms relative error of the group no. n, and tn is the total number of data groups. A small value of ER_{avg} indicates good overall accuracy of the wave model.

The rms relative error of each data group (ER_g) is defined as

$$ER_g = 100 \times \sqrt{\frac{\sum_{i=1}^{nc}(H_{ci} - H_{mi})^2}{\sum_{i=1}^{nc} H_{mi}^2}}, \tag{16}$$

where i is the wave height number, H_{ci} is the computed significant wave height of number i, H_{mi} is the measured significant wave height of number i, and nc is the total number of measured significant wave heights in each data group.

The question of how good a model is usually defined in a qualitative ranking (e.g., excellent, very good, good, fair, and poor). As the error of some existing irregular wave models is in the range of 7–21% (please see Rattanapitikon, 2007, Table 2), the qualification of error ranges of an irregular wave model may be classified into five ranges (i.e., excellent ($ER_g < 5.0$), very good ($5.0 \leqslant ER_g < 10.0$), good ($10.0 \leqslant ER_g < 5.0$), fair ($15.0 \leqslant ER_g < 20.0$), and poor ($ER_g \geqslant 20.0$)) and the acceptable error should be less than 10%.

The transformation of the significant wave height from the models MD1–MD6 is determined by taking numerical integration from offshore to shoreline. The energy dissipation is set to be zero when $H_s < H_{sb}$. The incipient wave breaking (H_{sb}) is computed from Eq. (14). The forward finite difference scheme is used to solve the differential equations. The length step (Δx) is set to be equal to the length between the points of measured wave heights, except if $\Delta x > 5$ m, Δx is set to be 5 m. The length steps (Δx) used in the present study are 0.2–1.5 m for small-scale experiments and 2.1–5.0 m for large-scale experiments.

Using the coefficients K_1–K_{10} which were proposed for regular waves, errors of the models MD1–MD6 on predicting H_s for two groups of experiment-scales are shown in Table 3. It can be seen from Table 3 that all models give unacceptable results in simulating the significant wave height transformation. This is a confirmation of the findings of the previous researchers. The unacceptable results may be due to: (1) the incipient breaking point of regular wave and irregular wave may not be the same point and (2) the amount of energy dissipation of regular waves and irregular waves may not be the same. Therefore, the prediction may be more accurate if the coefficients (K_1–K_{10}) are re-calibrated by using the significant wave height data.

4.2. Model calibration and selection

A calibration of each model is conducted by varying the coefficients (K_1–K_{10}) in the model until the minimum error (ER_{avg}) between measured and computed significant wave heights is obtained. The optimum values of K_1–K_{10} are shown in the second column of Table 4. The errors of models MD1–MD6 on simulating H_s for two groups of experiment-scales are shown in the third–fifth columns of Table 4. The examination results from Table 4 can be summarized as follows:

(a) The accuracy of all models is improved significantly after calibration.
(b) For small-scale wave flumes, the models MD3, MD5, and MD6 give very good predictions ($5.0 \leqslant ER_g < 10.0$), while the other models (MD1, MD2, and MD4) give good predictions ($10.0 \leqslant ER_g < 15.0$). The accuracy levels of the models in descending order are MD6, MD3, MD5, MD2, MD4, and MD1.
(c) For large-scale wave flumes, all models give very good predictions ($5.0 \leqslant ER_g < 10.0$). The accuracy levels of the models in descending order are MD5, MD6, MD2, MD3, MD4, and MD1.
(d) The overall accuracy levels of the models in descending order are MD5, MD6, MD3, MD2, MD4, and MD1.
(e) The models MD3, MD5, and MD6 give very good predictions ($5.0 \leqslant ER_g < 10.0$) for both small- and large-scale experiments. These models can be used for computing the significant wave height transformation. However, lesser error is better. The models MD5 and MD6 give almost the same accuracy and are more accurate than the others.
(f) The average error (ER_{avg}) of the models MD5 and MD6 are 7.5% and 7.6%, respectively. These numbers confirm in a quantitative sense the high degree of realism generated by the models. This means that the significant wave representation method is acceptable for computing the significant wave height transformation across-shore.

Overall, the models MD5 and MD6 give nearly the same accuracy. It may be interesting to look at the comparison in more detail. Table 5 shows the errors (ER_g) of MD5 and MD6 for 36 groups of test series. It can be seen from Table 5 that the models MD5 and MD6 give nearly the same overall accuracy (ER_{avg} of MD5 = 7.7% and ER_{avg} of MD6 = 7.6%). As the average errors (ER_{avg}) of models MD5 and MD6 from Tables 4 and 5 are almost the same, it is difficult to judge which model is better than the other. Evaluation of these two models may have to be based on their simplicity.

Substituting the calibrated coefficients $K_6 = 0.09$, $K_7 = 1.07$, $K_8 = 0.09$, $K_9 = 0.076$, and $K_{10} = 0.076$ into the corresponding equations (Eqs. (12)–(14)), the irregular wave models (MD5 and MD6) for computing H_s can be expressed as

$$\text{MD5}: \quad \frac{\rho g}{8}\frac{\partial(H_s^2 c_g)}{\partial x} = -0.09\frac{\rho g c}{8h} \times \left[H_s^2 - \left(1.07h\exp\left(-0.36 - \frac{1.25h}{\sqrt{LH_s}}\right)\right)^2\right], \tag{17}$$

$$\text{MD6}: \quad \frac{\rho g}{8}\frac{\partial(H_s^2 c_g)}{\partial x} = -0.09\frac{\rho g c_g}{8h}[H_s^2 - (0.076L\tanh(kh))^2], \tag{18}$$

Table 5
The errors (ER_g and ER_{avg}) of the models MD5– MD6 (using the calibrated coefficients) and the modified model (MD7) for 36 groups of test series

Sources	Test series	MD5	MD6	MD7
Hurue (1990)	Hu1	7.6	5.9	6.2
Smith and Kraus (1990)	R2000	11.7	7.5	6.6
	R22xx	12.0	11.3	9.9
	R6000	7.3	5.0	5.9
	R62xx	10.3	10.9	9.3
	R8000	3.8	4.6	4.2
	R82xx	10.4	10.8	8.8
Katayama (1991)	Ka1&Ka2	8.0	9.0	9.7
Ting (2001)	Ti1	4.8	3.1	3.1
Kraus and Smith (1994)	ST10	6.8	4.8	4.8
	ST20	5.4	5.2	5.0
	ST30	6.5	6.4	6.4
	ST40	8.3	8.4	8.3
	ST50	7.0	7.2	6.9
	ST60	8.3	8.6	7.9
	ST70	7.2	6.8	6.3
	ST80	9.6	9.4	8.9
	ST90	5.2	5.5	4.5
	STAO	5.7	4.9	4.3
	STCO	13.1	11.4	11.6
	STDO	10.1	10.7	10.4
	STJO	10.6	10.9	9.6
	STKO	21.7	21.4	20.9
Dette et al. (1998)	A8	10.9	13.0	12.3
	A9	2.9	4.9	5.1
	B1	7.6	9.1	8.1
	B2	4.2	4.5	4.2
	C1	9.9	11.5	10.4
	C2	4.0	4.8	4.7
	H1	4.4	5.4	6.1
	H2	4.8	4.3	3.7
	D1&D3	9.0	9.8	9.6
	D2	4.3	5.4	5.7
	E	3.2	4.0	4.4
	F	3.6	3.9	4.0
	G	6.4	5.1	5.8
Average error (ER_{avg})		7.7	7.6	7.3

Table 4
The errors (ER_g and ER_{avg}) of the models MD1– MD6 (using the calibrated coefficients) and the modified model (MD7) for two groups of experiment-scales (measured data from Table 2)

Models	Coefficients	ER_g		ER_{avg}
		Small-scale	Large-scale	
MD1 (Eq. (9))	$K_1 = 0.34$, $K_{10} = 0.098$	13.5	8.4	10.9
MD2 (Eq. (10))	$K_2 = 0.53$, $K_{10} = 0.098$	11.9	6.5	9.2
MD3 (Eq. (11))	$K_3 = 0.40$, $K_{10} = 0.098$	9.4	6.8	8.1
MD4 (Eq. (12))	$K_4 = 0.09$, $K_5 = 0.42$, $K_{10} = 0.076$	12.2	7.1	9.6
MD5 (Eq. (13))	$K_6 = 0.09$, $K_7 = 1.07$, $K_{10} = 0.076$	9.5	5.5	7.5
MD6 (Eq. (14))	$K_8 = 0.09$, $K_9 = 0.076$, $K_{10} = 0.076$	9.3	5.8	7.6
MD7 (Eq. (26))	$K_{11} = 0.095$, $K_{12} = -0.263$, $K_{13} = 0.179$	8.1	5.7	6.9

in which the incipient wave breaking or the starting point to include the energy dissipation into the models is determined from the following formula:

$$H_{sb} = 0.076L \tanh(kh). \tag{19}$$

The energy dissipation of MD5 and MD6 is zero when the stable wave height (the second term on the right-hand side of Eqs. (17) and (18)) is greater than the significant wave height. It can be seen that the stable wave height of MD6 (second term on the right-hand side of Eq. (18)) is the same as the formula that is used for computing the breaker height (Eq. (19)). This means that it is not necessary to check the incipient wave breaking. Eq. (18) can be used to compute the significant wave heights for the entire zone (from offshore to shoreline). This makes the model MD6 simpler than the model MD5. In terms of accuracy and simplicity, the model MD6 is the best and is recommended for computing the significant wave height transformation across-shore. As the model MD6 (Eq. (18)) is very simple, it may also serve as a reference model to test more complicated models against.

5. Model modification

Although, the model MD6 gives very good predictions, it may be modified to achieve even greater accuracy. The energy dissipation term in model MD6 is derived from the regular wave model of Rattanapitikon et al. (2003), which was developed based on the stable energy concept of Dally et al. (1985). The model MD6 (Eq. (18)) can be re-written as

$$\frac{\rho g}{8}\frac{\partial(H_s^2 c_g)}{\partial x} = -\frac{\rho g H_s^2 c_g}{8h}\left[0.09 - 0.09\left(\frac{H_{sb}}{H_s}\right)^2\right], \tag{20}$$

in which H_{sb} is calculated from Eq. (19). It can be seen that the energy dissipation term on the right-hand side of Eq. (20) can be written in a general form as a product of energy flux per unit depth and a dimensionless function (f) as

$$\frac{\rho g}{8}\frac{\partial(H_s^2 c_g)}{\partial x} = -\frac{\rho g H_s^2 c_g}{8h} f\left\{\frac{H_{sb}}{H_s}\right\}, \tag{21}$$

where f is a function of H_{sb}/H_s. The function f may be considered as a fraction of energy dissipation, while the energy flux per unit depth may be considered as a potential rate of energy dissipation. The function f of the stable energy concept (MD6) can be expressed as

$$f = -0.09\left(\frac{H_{sb}}{H_s}\right)^2 + 0.09 \quad \text{for } \frac{H_{sb}}{H_s} \leqslant 1.0, \tag{22a}$$

$$f = 0 \quad \text{for } \frac{H_{sb}}{H_s} > 1.0. \tag{22b}$$

It should be noted that Eq. (20) (or Eqs. (22a) and (22b)) is derived based on the assumption that the energy dissipation rate is proportional to the difference between the energy flux per unit depth and the stable energy flux per unit depth. If the assumption is correct, the relationship between f and H_{sb}/H_s should be a concave-down shape (since $d^2f/d(H_{sb}/H_s)^2$ is a negative value). It may be worthwhile to check this assumption through the relationship between f and H_{sb}/H_s. The data for plotting the relationship are the measured data of f and H_{sb}/H_s. The measured

Using a forward finite difference scheme to describe the wave model (Eq. (21)), the formula for determining measured f is expressed as

$$f_j = -\frac{(H_{s,j+1}^2 c_{g,j+1} - H_{s,j}^2 c_{g,j})}{(x_{j+1} - x_j)}\frac{h_j}{H_{s,j}^2 c_{g,j}}, \tag{23}$$

where j is the grid number. Hereafter, the variable f determined from Eq. (23) is referred to as the measured f.

The required data set for plotting the relationship between f and H_{sb}/H_s is the measured data of h, T_p, H_s, and x. The computation of other related variables (e.g., L, k, and c_g) is based on linear wave theory. The breaker height (H_{sb}) is determined from Eq. (19). To avoid a large fluctuation in the relationship, the data of wave height variation across-shore should have a small fluctuation.

Because of a small fluctuation of wave height variation across-shore, the data from Dette et al. (1998) are used for plotting the relationship between measured f and H_{sb}/H_s. The relationship between measured f and H_{sb}/H_s is shown in Fig. 1. The line of computed f from Eqs. (22a) and (22b) is shown as the dotted line in Fig. 1. It can be seen that Eqs. (22a) and (22b) are fitted reasonably well to the measured f. However, the shape of measured f tends to be concave-up instead of concave-down as Eqs. (22a) and (22b) suggests it should. It seems to be better to fit f with a quadratic equation as

$$f = K_{11}\left(\frac{H_{sb}}{H_s}\right)^2 + K_{12}\left(\frac{H_{sb}}{H_s}\right) + K_{13}, \tag{24}$$

where K_{11}–K_{13} are the coefficients. From the multi-regression analysis (between measured f and H_{sb}/H_s) by using the data that $H_{sb}/H_s \leqslant 1.0$, the values of K_{11}–K_{13} are 0.09, −0.26, and 0.17, respectively. The best-fitted line is shown as the solid line in Fig. 1. However, the values of K_{11}–K_{13} are not used in the wave model because the values of K_{11}–K_{13} are optimum only for the data of Dette et al. (1998), and they may change slightly when applying to all collected laboratory data.

Substituting Eq. (24) into Eq. (21), the general form of the modified model can be expressed as

$$\text{MD7}: \quad \frac{\rho g}{8}\frac{\partial(H_s^2 c_g)}{\partial x} = -\frac{\rho g H_s^2 c_g}{8h}\left[K_{11}\left(\frac{H_{sb}}{H_s}\right)^2 + K_{12}\left(\frac{H_{sb}}{H_s}\right) + K_{13}\right]. \tag{25}$$

The collected irregular wave data shown in Table 2 are used to calibrate the model MD7 (Eq. (25)). The wave height transformation is computed by numerical integration of the model MD7 (Eq. (25)). The forward finite difference scheme is used to solve the model. The calibration of the model is conducted by varying

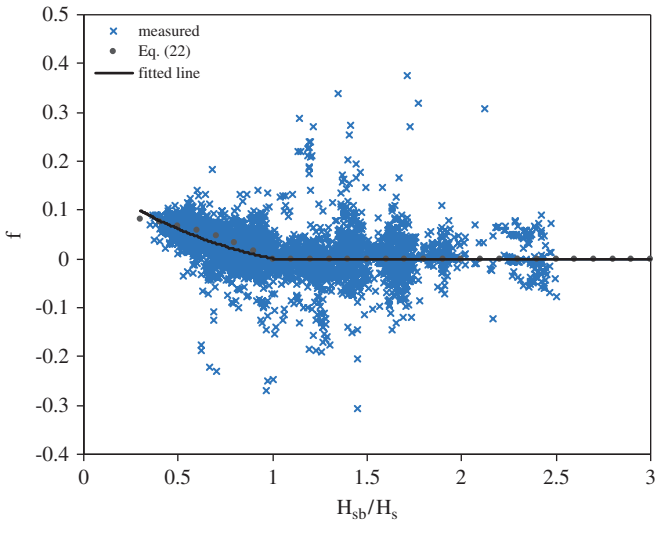

Fig. 1. Relationship between f and H_{sb}/H_s (measured data from Dette et al., 1998).

the values of K_{11}–K_{13} until the minimum error (ER_{avg}) of the model is obtained. The optimum values of K_{11}–K_{13} are 0.095, −0.263, and 0.179, respectively. The errors (ER_g and ER_{avg}) of model MD7 are shown in the last row of Table 4 and the last column of Table 5. It can be seen from Tables 4 and 5 that the model MD7 gives the best predictions.

To gain an impression of overall performance of the modified model (MD7) for computing H_s, the results of model MD7 are plotted against the measured data. Comparison between measured and computed significant wave heights from the model MD7 for all cases are shown in Fig. 2. Examples of computed significant wave height transformation across-shore are shown in Figs. 3 and 4. Case numbers in Figs. 3 and 4 are kept to be the same as the originals. Overall, it can be seen that the model MD7 gives a quite realistic simulation of the significant wave height transformation across-shore. However, the present model has certain limitations, which may restrict its use. The limitations of the model MD7 can be listed as follows:

(a) The model gives the worst prediction for the case of broad-crested mound ($ER_g = 20.9\%$, see test no. STKO in Table 5). The main error is caused by a sharp drop in measured wave height at a distance of $x = 44.2$ m on top of the bar (see Fig. 4d). This sharp drop occurred in all cases of the test no. STKO (at $x = 44.2$ m). It is difficult to find out the reason for such a sharp drop in the wave height.

(b) The model gives only good predictions ($ER_g \approx 10\%$) for the wave on the barred beach or narrow-crested mound (see test no. R22xx, R62xx, R82xx, Ka1&Ka2, and STJO in Table 5; see also Figs. 3c–g and 4c). The model could not predict the rapid increase and decrease in wave heights near the bar. The model tends to give over prediction for the wave heights around the trough of narrow-bar (see Fig. 3c–e) while it tends to give under prediction around the trough of the broad-bar (see Fig. 3f and g).

(c) As the model MD7 (Eq. (25)) is an empirical model, its validity may be limited according to the range of experimental conditions which were employed in the calibration. The present formula should be applicable for deepwater wave steepness (H_{so}/L_o) ranging between 0.002 and 0.064.

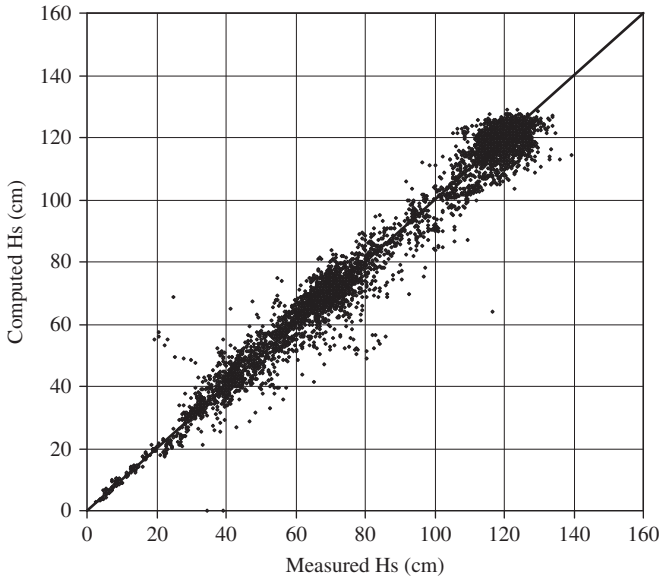

Fig. 2. Comparison between measured and computed significant wave height by using the model MD7 (measured data from Table 2).

(d) It is not clear, whether the model can be applied to the ocean or not because the model is not verified by the field data. However, it has a high possibility to apply the model to the coasts or oceans because the large-scale experiments have a scale approximately the same as the conditions in the oceans. Moreover, it was shown by some researchers (e.g., Wise et al., 1996; Rattanapitikon and Shibayama, 1998) that the models, which were developed based on large-scale experiments, could be applied directly to the real ocean waves.

As shown in Section 4 that the regular wave model for computing H can be applied directly for computing H_s, it is expected that the irregular wave model for computing H_s should also be applicable for computing H. The model MD7 (Eq. (25)) is applied to regular waves as

$$\text{MD8}: \quad \frac{\rho g}{8}\frac{\partial(H^2 c_g)}{\partial x} = -\frac{\rho g H^2 c_g}{8h}\left[K_{14}\left(\frac{H_b}{H}\right)^2 + K_{15}\left(\frac{H_b}{H}\right) + K_{16}\right], \tag{26}$$

where K_{14}–K_{16} are the coefficients which can be determined from model calibration and H_b is the breaker height of the regular waves which is determined from the breaking criterion of Miche (1944).

The collected regular wave data shown in Table 1 are used to calibrate the model MD8 (Eq. (26)). The wave height transformation is computed by numerical integration of the model MD8. The forward finite difference scheme is used to solve the model. The calibration of the model is conducted by varying the values of K_{14}–K_{16} until the minimum error (ER_{avg}) of the model is obtained. The optimum values of K_{14}–K_{16} are 0.010, −0.128, and 0.226, respectively. The errors (ER_g and ER_{avg}) of the model MD8 and the existing regular wave models (shown in Section 3) are shown in Table 6. It can be seen from Table 6 that it is possible to use the model MD8 for computing regular wave heights transformation.

Substituting the calibrated coefficients K_{11}–K_{16} into Eqs. (25) and (26), the modified models for irregular and regular waves can be expressed as

$$\text{MD7}: \quad \frac{\rho g}{8}\frac{\partial(H_s^2 c_g)}{\partial x} = -\frac{\rho g H_s^2 c_g}{8h} \times \left[0.095\left(\frac{H_{sb}}{H_s}\right)^2 - 0.263\left(\frac{H_{sb}}{H_s}\right) + 0.179\right], \tag{27}$$

$$\text{MD8}: \quad \frac{\rho g}{8}\frac{\partial(H^2 c_g)}{\partial x} = -\frac{\rho g H^2 c_g}{8h} \times \left[0.010\left(\frac{H_b}{H}\right)^2 - 0.128\left(\frac{H_b}{H}\right) + 0.226\right]. \tag{28}$$

6. Conclusions

This study was carried out to investigate the possibility of using the significant wave representation method. The significant wave height transformation across-shore was computed from the energy flux conservation. The selected six regular wave models were directly applied to the irregular waves (by using significant wave height and spectral peak period) to investigate their applicability for simulating significant wave height transformation. The breaking criterion of Miche (1944) was applied to compute the incipient breaker height. Laboratory data from small- and large-scale wave flumes were used to calibrate and examine the models. It was found that three regular wave models (with new coefficients) can be used for computing the significant wave heights with very good accuracy (i.e., the models MD3, MD5, and

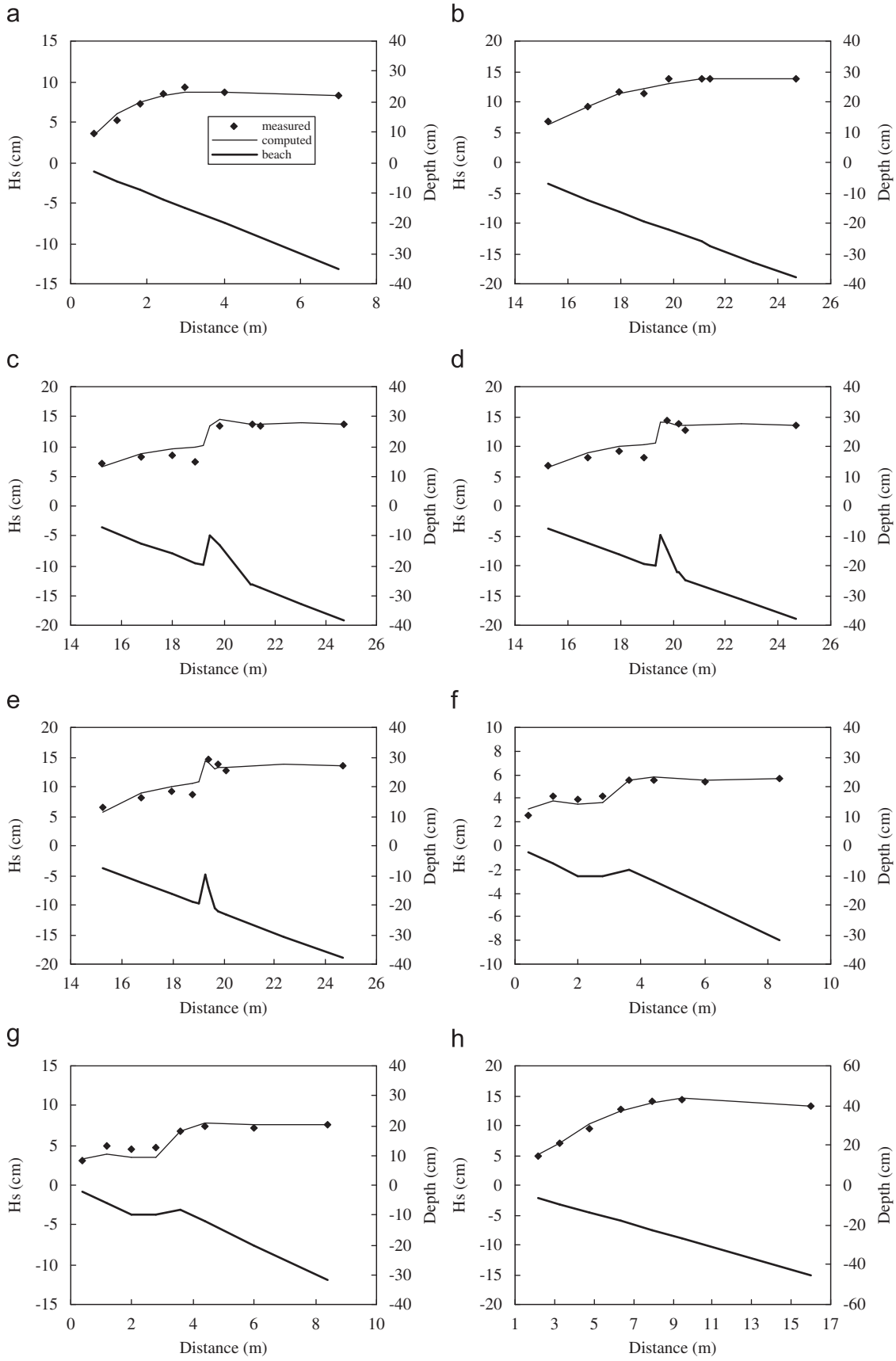

Fig. 3. Examples of measured and computed significant wave height transformation by using the model MD7 (measured data from small-scale experiments). (a) Hu1, (b) R8000, (c) R8210, (d) R8220, (e) R8230, (f) Ka1, (g) Ka2 and (h) Ti1.

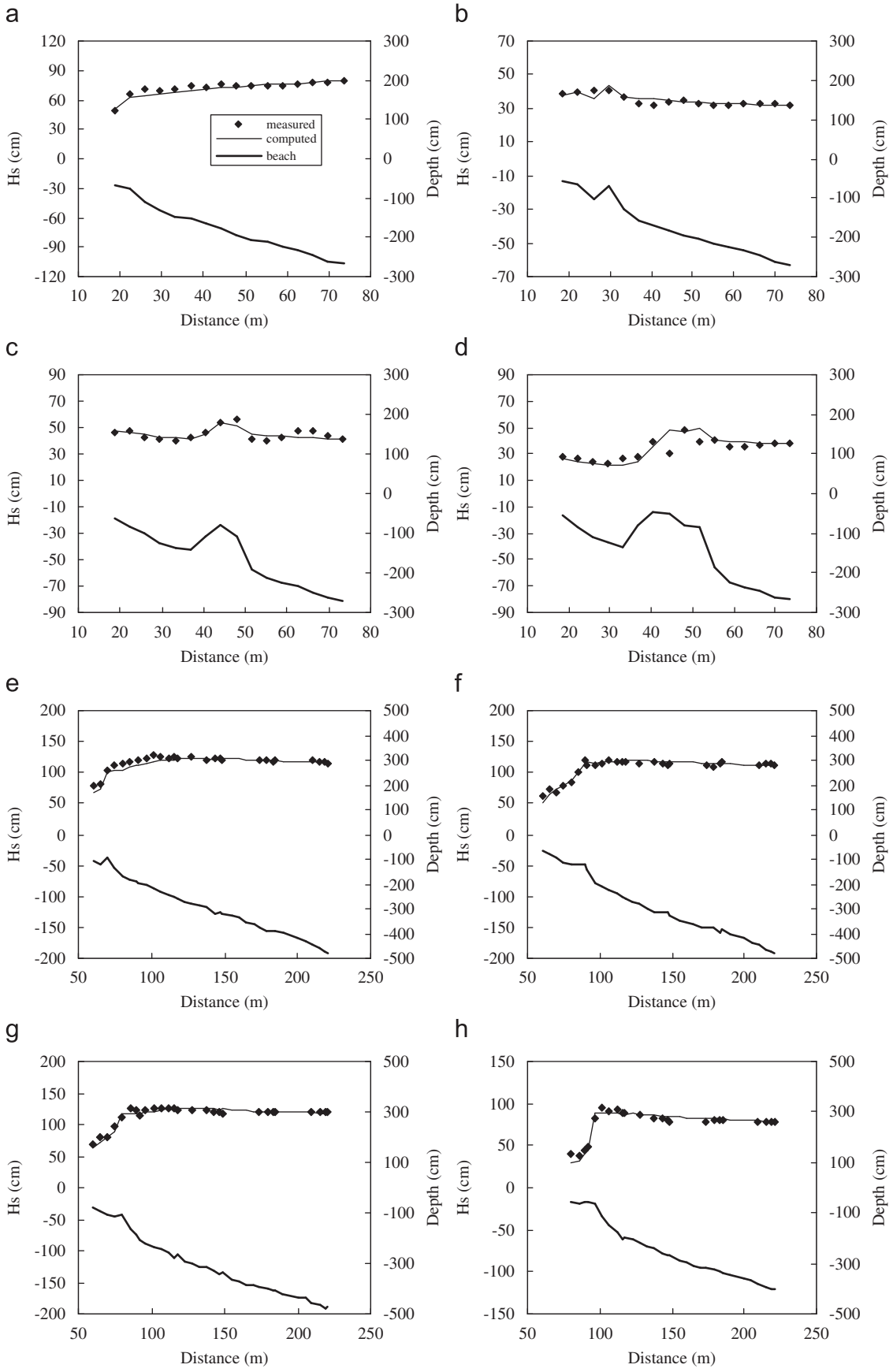

Fig. 4. Examples of measured and computed significant wave height transformation by using the model MD7 (measured data from large-scale experiments) (a) ST10:a0515a, (b) ST30:a1409a, (c) STJO:S1008a, (d) STKO:S1217a, (e) A9:17129602, (f) C2:14039701, (g) F:17079701 and (h) G: 07089701.

Table 6
The errors (ER_g and ER_{avg}) of the six existing regular wave and the modified model (MD8) for two groups of experiment-scales (measured data from Table 1)

Regular wave models	ER_g		ER_{avg}
	Small-scale	Large-scale	
Battjes and Janssen (1978)	34.4	49.0	41.7
Thornton and Guza (1983)	22.1	26.0	24.0
Deigaard et al. (1991)	23.2	23.1	23.1
Dally et al. (1985)	17.3	20.2	18.8
Rattanapitikon and Shibayama (1998)	16.3	16.6	16.4
Rattanapitikon et al. (2003)	16.3	17.7	17.0
MD8	15.9	17.5	16.7

MD6). This leads to the conclusion that the concept of significant wave representation method can be used for computing the significant wave height transformation across-shore. On the strength of both accuracy and simplicity of the three possible models, the model MD6 is recommended for use as the best method for computing the significant wave height transformation across-shore.

Although, the model MD6 gives very good predictions, it can be modified to achieve better predictions. The model MD6 can be rewritten as a product of energy flux per unit depth and dimensionless function ($f\{H_{sb}/H_s\}$). The modification is performed by deriving the new formula of function f. The general form of f is derived from plotting the relationship between measured f and H_{sb}/H_s. The shape of measured f trends to be concave-up and can be fitted with a quadratic equation. All collected data were used in the study to calibrate and examine the modified model. Compared with the three possible models (MD3, MD5, and MD6), the modified model gives the best prediction. The modified model (with different coefficients) can also be applied to predict the regular wave height transformation. As the modified model is an empirical model, its validity may be limited depending on the range of experimental conditions that are employed in the calibration. The model should be applicable for deepwater wave steepness (H_{so}/L_o) ranging between 0.002 and 0.064.

Acknowledgment

This research was sponsored by the Thailand Research Fund and the Commission on Higher Education, Ministry of Education.

Appendix. Governing equation of the significant wave representation method

Considering average energy flux of an irregular wave train (based on linear wave theory),

$$\overline{Ec_g} = \frac{\sum_{i=1}^{N}(E_i c_{gi})}{N} = \frac{1}{8}\rho g \frac{\sum_{i=1}^{N} H_i^2 c_{gi}}{N}, \tag{A.1}$$

where $\overline{Ec_g}$ is the average energy flux of an irregular wave train, E_i is the energy density for the ith individual wave, c_{gi} is the group velocity for the ith individual wave, H_i is the wave height for the ith individual wave, and N is the total number of waves in the irregular wave train.

The Rayleigh distribution serves as a good engineering formula for the distribution of zero-crossing wave heights as demonstrated by many researchers (e.g., Goodknight and Russel, 1963; Goda, 1974; Thornton and Guza, 1983; and Rattanapitikon and Shibayama, 2007). To simplify the analysis, the wave heights are assumed to follow the Rayleigh distribution (narrow-banded in frequency) so that the individual waves have almost the same period and consequently almost the same group velocity (c_g). Therefore, Eq. (A.1) can be simplified to be

$$\overline{Ec_g} = \frac{1}{8}\rho g c_g \frac{\sum_{i=1}^{N} H_i^2}{N}. \tag{A.2}$$

The spectral peak period (T_p) is usually used to compute the group velocity because it is typically reported for the irregular wave data.

Since $\sqrt{\sum_{i=1}^{N} H_i^2/N}$ is equal to the root mean square wave height (H_{rms}), Eq. (A.2) can be written in terms of H_{rms} as

$$\overline{Ec_g} = \frac{1}{8}\rho g H_{rms}^2 c_g. \tag{A.3}$$

The average energy flux conservation of the irregular wave train can be written as

$$\frac{\partial(\overline{Ec_g})}{\partial x} = -\overline{D_B}, \tag{A.4}$$

where $\overline{D_B}$ is the average energy dissipation.

Substituting Eq. (A.3) into Eq. (A.4), the energy flux conservation of the representative wave approach can be expressed as

$$\frac{1}{8}\rho g \frac{\partial(H_{rms}^2 c_g)}{\partial x} = -\overline{D_B}. \tag{A.5}$$

It should be noted that Eq. (A.5) is developed based on linear wave theory and Rayleigh distribution. This crude assumption of the representative wave approach may not be theoretically justified. However, there are many wave models that are successful in using the energy flux conservation (Eq. (A.5)) for computing H_{rms}, e.g., the models of Battjes and Janssen (1978), Thornton and Guza (1983), Larson (1995), Baldock et al. (1998), Ruessink et al. (2003), and Rattanapitikon (2007). Therefore, Eq. (A.5) seems be acceptable for computing H_{rms}.

If the energy flux conservation of the representative wave (Eq. (A.5)) can be used for computing H_{rms}, it may be possible to be used for computing H_s because H_{rms} can be converted to H_s through the known coefficient (i.e., $H_s = \beta H_{rms}$, in which $\beta = 1.42$ for the Rayleigh distribution).

Substituting $H_s = \beta H_{rms}$ into Eq. (A.5), the governing equation of the significant wave representation method can be written as

$$\frac{1}{8}\rho g \frac{\partial(H_s^2 c_g)}{\partial x} = -\overline{D_{Bs}}, \tag{A.6}$$

where $\overline{D_{Bs}} = \beta^2 \overline{D_B}$.

References

Andreas, E.L., Wang, S., 2007. Predicting significant wave height off the northeast coast of the United States. Ocean Engineering 34 (8–9), 1328–1335.
Baldock, T.E., Holmes, P., Bunker, S., Van Weert, P., 1998. Cross-shore hydrodynamics within an unsaturated surf zone. Coastal Engineering 34, 173–196.
Battjes, J.A., Groenendijk, H.W., 2000. Wave height distributions on shallow foreshores. Coastal Engineering 40, 161–182.
Battjes, J.A., Janssen, J.P.F.M., 1978. Energy loss and set-up due to breaking of random waves. In: Proceedings of the 16th Coastal Engineering Conference, ASCE, pp. 569–589.
Bouws, E., Gunther, H., Rosenthal, W., Vincent, C.L., 1985. Similarity of the wind wave spectrum in finite depth water. Journal of Geophysical Research 90 (C1), 975–986.
Bretschneider, C.L., 1968. Significant waves and wave spectrum. Ocean Industry (February), 40–46.
Bruun, P., 1954. Coastal erosion and development of beach profiles. Technical Memorandum No. 44, US Army Beach Erosion Board, US Army Corps of Engineers.
Cox, T., Kobayashi, N., 1997. Kinematic undertow model with logarithmic boundary layer. Journal of Waterway, Port, Coastal and Ocean Engineering, ASCE 123 (6), 354–360.
Dally, W.R., 1992. Random breaking waves: field verification of a wave-by-wave algorithm for engineering application. Coastal Engineering 16, 369–397.

Dally, W.R., Dean, R.G., Dalrymple, R.A., 1985. Wave height variation across beaches of arbitrary profile. Journal of Geophysical Research 90 (C6), 11917–11927.
Deigaard, R., Justesen, P., Fredsoe, J., 1991. Modelling of undertow by a one-equation turbulence model. Coastal Engineering 15, 431–458.
Dette, H.H., Peters, K., Newe, J., 1998. MAST III—SAFE Project: Data Documentation, Large Wave Flume Experiments '96/97. Report No. 825 and 830, Leichtweiss Institute, Technical University Braunschweig, Germany.
Goda, Y., 1974. Estimation of wave statistics from spectral information. In: Proceedings of the Ocean Waves Measurement and Analysis Conference, ASCE, pp. 320–337.
Goda, Y., 2000. Random Seas and the Design of Maritime Structures. World Scientific Publishing Co. Pte. Ltd., Singapore.
Goda, Y., 2004. A 2-D random wave transformation model with gradational breaker index. Coastal Engineering Journal, JSCE 46 (1), 1–38.
Goodknight, R.C., Russel, T.L., 1963. Investigation of the statistics of wave heights. Journal of Waterways and Harbors Division, ASCE 89 (WW2), 29–55.
Hansen, J.B., Svendsen, I.A., 1984. A theoretical and experiment study of undertow. In: Proceedings of the 19th Coastal Engineering Conference, ASCE, pp. 2246–2262.
Hasselmann, K., Barnett, T.P., Bouws, E., Carlson, H., Cartwright, D.E., Enke, K., Ewing, J.A., Gienapp, H., Hasselmann, D.E., Kruseman, P., Meerburg, A., Müller, P., Olbers, D.J., Richter, K., Sell, W., Walden, H., 1973. Measurements of wind–wave growth and swell decay during the Joint North Sea Wave Project (JONSWAP). Deutsche Hydrographische Zeitschrift A 8 (12), 1–95.
Horikawa, K., Kuo, C.T., 1966. A study of wave transformation inside the surf zone. In: Proceedings of the 10th Coastal Engineering Conference, ASCE, pp. 217–233.
Hurue, M., 1990. Two-dimensional distribution of undertow due to irregular waves. B.Eng. Thesis, Department of Civil Engineering, Yokohama National University, Japan (in Japanese).
Kajima, R., Shimizu, T., Maruyama, K., Saito, S., 1983. On-offshore sediment transport experiment by using large scale wave flume. Collected Data No. 1–8, Central Research Institute of Electric Power Industry, Japan (in Japanese).
Katayama, H., 1991. Cross-shore velocity distribution due to breaking of irregular waves on a bar-type beach. B.Eng. Thesis, Department of Civil Engineering, Yokohama National University, Japan (in Japanese).
Kraus, N.C., Smith, J.M., 1994. SUPERTANK Laboratory Data Collection Project, vols. 1–2. Technical Report CERC-94-3, WES, US Army Corps of Engineers.
Kuriyama, Y., 1996. Model of wave height and fraction of breaking waves on a barred beach. In: Proceedings of the 25th Coastal Engineering Conference, ASCE, pp. 247–259.
Larson, M., 1995. Model for decay of random waves in surf zone. Journal of Waterway, Port, Coastal, and Ocean Engineering, ASCE 121 (1), 1–12.
Longuet-Higgins, M.S., 1952. On the statistical distribution of the heights of sea waves. Journal of Marine Research 11 (3), 246–266.
Miche, R., 1944. Mouvements ondulatoires des mers en profondeur constante on decroissante. Ann. des Ponts et Chaussees, Chapter 114, pp. 131–164, 270–292, and 369–406.
Mitsuyasu, H., 1970. On the growth of spectrum of wind-generated waves (2)—spectral shape of wind waves at finite fetch. In: Proceedings of the 17th Japanese Conference on Coastal Engineering, pp. 1–7 (in Japanese).
Mizuguchi, M., 1982. Individual wave analysis of irregular wave deformation in the nearshore zone. In: Proceedings of the 18th Coastal Engineering Conference, ASCE, pp. 485–504.
Nadaoka, K., Kondoh, T., Tanaka, N., 1982. The structure of velocity field within the surf zone revealed by means of laser-doppler anemometry. Report of the Port and Harbor Research Institute 21 (2), pp. 50–102 (in Japanese).
Nagayama, S., 1983. Study on the change of wave height and energy in the surf zone. B.Eng. Thesis, Department of Civil Engineering, Yokohama National University, Japan (in Japanese).
Okayasu, A., Shibayama, T., Horikawa, K., 1988. Vertical variation of undertow in the surf zone. In: Proceedings of the 21st Coastal Engineering Conference, ASCE, pp. 478–491.
Rattanapitikon, W., 2007. Calibration and modification of energy dissipation models for irregular waves breaking. Ocean Engineering 34 (11–12), 1592–1601.
Rattanapitikon, W., Shibayama, T., 1998. Energy dissipation model for regular and irregular breaking waves. Coastal Engineering Journal, JSCE 40 (4), 327–346.
Rattanapitikon, W., Shibayama, T., 2007. Estimation of shallow water representative wave heights. Coastal Engineering Journal, JSCE 49 (3), 291–310.
Rattanapitikon, W., Karunchintadit, R., Shibayama, T., 2003. Irregular wave height transformation using representative wave approach. Coastal Engineering Journal, JSCE 45 (3), 489–510.
Ruessink, B.G., Walstra, D.J.R., Southgate, H.N., 2003. Calibration and verification of a parametric wave model on barred beaches. Coastal Engineering 48, 139–149.
Sato, S., Fukuhama, M., Horikawa, K., 1988. Measurement of near-bottom velocities in random waves on a constant slope. Coastal Engineering in Japan, JSCE 31 (2), 219–229.
Sato, S., Isayama, T., Shibayama, T., 1989. Long-wave component in near-bottom velocity under random waves on a gentle slope. Coastal Engineering in Japan, JSCE 32 (2), 149–159.
Shibayama, T., Horikawa, K., 1985. Numerical model for two-dimensional beach transformation. In: Proceedings of the Japan Society of Civil Engineers, No. 357/II-3 (Hydraulic and Sanitary), pp. 167–176.
Smith, J.M., Kraus, N.C., 1990. Laboratory study on macro-features of wave breaking over bars and artificial reefs. Technical Report CERC-90-12, WES, US Army Corps of Engineers.
Thornton, E.B., Guza, R.T., 1983. Transformation of wave height distribution. Journal of Geophysical Research 88 (C10), 5925–5938.
Ting, F.C.K., 2001. Laboratory study of wave and turbulence velocity in broad-banded irregular wave surf zone. Coastal Engineering 43, 183–208.
Tucker, M.J., Pitt, E.G., 2001. Waves in Ocean Engineering. Elsevier Ocean Engineering Book Series, vol. 5. Elsevier, Amsterdam.
Wise, R.A., Smith, S.J., Larson, M., 1996. SBEACH: Numerical model for simulating storm-induced beach change. Report 4: Cross-Shore Transport Under Random Waves and Model Validation with SUPERTANK and Field Data, Technical Report CERC-89-9, WES, US Army Corps of Engineers.

Songklanakarin J. Sci. Technol.
30 (3), ..., May - Jun. 2008

Songklanakarin Journal of Science and Technology
http://www.sjst.psu.ac.th

Original Article

Energy dissipation model for a parametric wave approach based on laboratory and field experiments

Winyu Rattanapitikon* and Sangapol Sawanggun

Civil Engineering Program, Sirindhorn International Institute of Technology, Thammasat University, Pathum Thani 12121, Thailand

Received .....; Accepted .....

Abstract

This study was undertaken to develop a simple energy dissipation model for computing the root mean square wave height transformation. The parametric wave approach of Battjes and Janssen (1978) was used as a framework for developing the energy dissipation model. In contrast to the common derivation, the fraction of breaking waves was not derived from the assumed probability density function of wave heights, but derived directly from the measured wave heights. The present model was verified extensively for a variety of wave and beach conditions (including small-scale, large-scale, and field experiments), and compared with four existing dissipation models. The present model gives very good accuracy for a wide range of wave and beach conditions and gives better predictions than those of existing models.

Keywords: irregular wave model, energy dissipation, parametric wave, surf zone

1. Introduction

Wave height is one of the most essential required factors for many coastal engineering applications such as the design of coastal structures and the study of beach morphodynamics. When waves propagate in shallow water, their profiles become steeper and they eventually break. Once the waves start to break, a part of the wave energy is transformed into turbulence and heat, and the wave height decreases towards the shore. The rate of energy dissipation of breaking waves is an essential requirement for computing wave height transformation in the surf zone. Several models have been proposed for computing the energy dissipation due to wave breaking, differing mainly in their formulation of the energy dissipation, and whether they were developed for regular (a single broken wave) or irregular waves.

Widely used models for computing the energy dissipation of a regular wave (a single broken wave) seem to be the bore model of Le Mehaute (1962) and the stable energy model of Dally *et al.* (1985). Brief reviews of these two models are described in the paper of Rattanapitikon and Leangruxa (2001). Aside from these two models, a number of alternative models for computing the energy dissipation have been presented. Horikawa and Kuo (1966) estimated the internal energy dissipation from the turbulent velocity fluctuations, which are assumed to decay exponentially with distance from the incipient wave breaking. Sawaragi and Iwata (1974) refined this approach by introducing the Prandt mixing length model to describe the turbulent velocity fluctuations. Mizuguchi (1980) applied an analytical solution for internal energy dissipation due to the viscosity, where the eddy viscosity replaces the molecular kinematic viscosity.

Irregular wave breaking is more complex than regular wave breaking. In contrast to regular waves, there is no well-defined breakpoint for irregular waves. The higher waves tend to break at a greater distance from the shore. Closer to the shore, more and more waves break, until almost all the waves break in the inner surf zone. The energy dissipation model developed for regular waves and extended to irregular waves introduces complexities, primarily with respect to the representation of the probability density function of wave

*Corresponding author.
Email address: winyu@siit.tu.ac.th

heights. Common methods to model irregular wave height transformations can be classified into four main approaches, i.e. representative wave approach, spectral approach, probabilistic approach, and parametric wave approach. For computing beach morphodynamics, the wave model should be kept as simple as possible because of the frequent updating of wave fields to account for the change of the bottom morphology. The parametric and representative wave approaches appear to be simple methods and seem to be suitable for being incorporated in the beach morphodynamic model.

For the representative wave approach, the regular wave model has been directly applied to irregular waves by using representative (or equivalent) waves, while the parametric approach considers the random nature of the waves but describes the energy dissipation rate in terms of time-averaged parameters. The parametric wave models were developed based on the assumed probability density function (*pdf*) of wave heights inside the surf zone. The average rate of energy dissipation is described by integrating the product of energy dissipation of a broken wave and the probability of occurrence of breaking waves. The parametric wave approach is expected to be better than the representative wave approach because it includes the random nature of the waves into the model while the other does not. Therefore, the present study focuses on the parametric wave approach.

The parametric wave models are generally based on the work of Battjes and Janssen (1978). The model relies on the macroscopic features of breaking waves and predicts only the transformation of root-mean-square (*rms*) wave height. The wave height transformation is computed from the energy flux conservation law. It is:

$$\frac{\partial\left(Ec_g\cos\theta\right)}{\partial x} = -D_B \tag{1}$$

where E is the wave energy density, c_g is the group velocity, θ is the mean wave angle, D_B is the distance in the cross shore direction, and is the energy dissipation rate due to wave breaking. The energy dissipation rate due to bottom friction is neglected. All variables are based on linear wave theory and Snell's law is employed to describe wave refraction.

From linear wave theory, the wave energy density (E) is equal to $\rho g H_{rms}^2/8$. Therefore, Equation 1 can be written in terms of wave height as:

$$\frac{\rho g}{8}\frac{\partial\left(H_{rms}^2 c_g\cos\theta\right)}{\partial x} = -D_B \tag{2}$$

where ρ is the density of water, g is the gravitational acceleration, H_{rms} and is the *rms* wave height.

The *rms* wave height transformation can be computed from the energy flux balance equation (Equation 2) by substituting the model of energy dissipation rate (D_B) and numerically integrating from offshore to the shoreline. In the offshore zone, the energy dissipation rate is set to zero. The main difficulty of Equation 2 is how to formulate the energy dissipation rate caused by the breaking waves.

During the past decades, various energy dissipation models for the parametric wave approach have been proposed for computing H_{rms} in the surf zone. Because of the complexity of the wave breaking mechanisms, most of the energy dissipation models were developed based on an empirical or semi-empirical approach. It is well known that the validity of an empirical formula may be limited according to the range of experimental conditions that were employed in the calibrations and verifications. To make an empirical formula reliable, it is necessary to calibrate and verify the formula with a large amount of data and a wide range of experimental conditions. Since many energy dissipation models were developed based on data with limited experimental conditions, there is still a need for more data to confirm the underlying assumptions in order to make the model more reliable. It is the purpose of this study to develop a simple energy dissipation model for the parametric wave approach based on a wide range of experimental conditions.

Experimental data of *rms* wave height transformation from 13 sources, covering 1723 cases of wave and beach conditions, have been collected for verifying the dissipation models. The experiments cover a wide range of wave and bottom topography conditions, including small-scale, large-scale, and field experiments. The experiments cover a variety of beach conditions (i.e. plane, barred, and sandy beaches) and a range of deepwater wave steepnesses (H_{rmso}/L_o) from 0.0007 to 0.0588. A summary of the collected experimental data is given in Table 1. Excluding the introduction and the conclusions, this paper is divided into three main parts. The first part briefly reviews some existing dissipation models for the parametric wave approach. The second part describes the development of the present model. The last part is the verification of the present model in comparison with the existing models.

2. Existing Energy Dissipation Models

During the past decades, various energy dissipation models have been developed based on a framework of the parametric wave approach of Battjes and Janssen (1978). Brief reviews of some existing dissipation models are described below.

a) Battjes and Janssen (1978), hereafter referred to as BJ78, proposed to compute D_B by multiplying the fraction of breaking waves (Q_B) by the energy dissipation of a single broken wave. The energy dissipation of a broken wave (D_{BS}) is determined from a simplified bore-type dissipation model and assumes that all broken waves have a height equal to the breaker height (H_b) as:

$$D_B = Q_{b1}\frac{\rho g H_b^2}{4T_p} \tag{3}$$

where Q_{b1} is the fraction of breaking waves of BJ78, and T_p is the spectral peak period. The fraction of breaking waves (Q_{b1}) was derived based on the assumption that the prob-

Table 1. Summary of collected experimental data.

Sources	Total no. of cases	Total no. of data	Beach conditions	H_{rmso}/L_o	Apparatus
Hurue (1990)	1	7	plane beach	0.0259	small-scale
Smith and Kraus (1990)	12	96	plane and barred beach	0.0214-0.0588	small-scale
Sultan (1995)	1	12	plane beach	0.0042	small-scale
Grasmeijer and Rijn (1999)	2	20	sandy beach	0.0142-0.0168	small-scale
Hamilton and Ebersole (2001)	1	10	plane beach	0.0165	small-scale
Ting (2001)	1	7	plane beach	0.0161	small-scale
Kraus and Smith (1994): SUPERTANK project	128	2,223	sandy beach	0.0011-0.0452	large-scale
Roelvink and Reniers (1995): LIP 11D project	95	923	sandy beach	0.0039-0.0279	large-scale
Dette *et al.* (1998): MAST III – SAFE project	138	3,559	sandy beach	0.0061-0.0147	large-scale
Thornton and Guza (1986)	4	60	sandy beach	0.0012-0.0013	field
Kraus *et al.* (1989): DUCK85 project	8	90	sandy beach	0.0007-0.0018	field
Birkemeier *et al.* (1997): DELILAH project	745	5,033	sandy beach	0.0007-0.0254	field
Herbers *et al.* (2006): DUCK94 project	587	6,102	sandy beach	0.0009-0.0290	field
Total	1,723	18,142		0.0007-0.0588	

ability density function of wave heights could be modeled with a Rayleigh distribution truncated at the breaker height (H_b) and all broken waves have a height equal to the breaker height. The result is:

$$\frac{1-Q_{b1}}{-\ln Q_{b1}} = \left(\frac{H_{rms}}{H_b}\right)^2 \tag{4}$$

in which the breaker height (H_b) is determined from the formula of Miche (1951) with the additional coefficient (γ) in the tan-hyperbolic function as:

$$H_b = 0.14L\tanh(\gamma kh) \tag{5}$$

where L is the wavelength related to T_p, k is the wave number, and h is the water depth. Based on their small-scale laboratory data, the coefficient γ is determined at 0.91. As Equation 4 is an implicit equation, it has to be solved for Q_{b1} either by an iterative technique (e.g. Newton-Raphson technique), or by a 1-D look-up table (Southgate and Nairn, 1993), or by fitting Q_{b1} with a polynomial function as:

$$Q_{b1} = \sum_{n=0}^{7} a_n \left(\frac{H_{rms}}{H_b}\right)^n \tag{6}$$

where a_n is the constant of n^{th} term. A multiple regression analysis is used to determine the constants a_0 to a_7. The correlation coefficient (R^2) of Equation 6 is 0.99999999. The values of the constants a_0 to a_7 are shown in Table 2. Equation 6 is applicable for $0.3 < H_{rms}/H_b < 1.0$. For $H_{rms}/H_b \leq 0.3$, the value of Q_{b1} is very small (less than 10^{-4}) and thus is set as zero. The value of Q_{b1} is set to be 1.0 when $H_{rms}/H_b \geq 1.0$. It should be noted that the two main assumptions for deriving the model (i.e. the assumptions of the simplified bore-type dissipation model and the truncated-Rayleigh distribution of wave heights) are not supported by the experimental data. However, the model has been used successfully in many applications for computing H_{rms} transformation (e.g. Johnson, 2006; and Oliveira, 2007).

Table 2. Values of constants a_0 to a_7 for computing Q_{b1}.

Constants	Values
a_0	0.231707207858562
a_1	-3.609582722187040
a_2	22.594833612442000
a_3	-72.536799430847200
a_4	126.870449066162000
a_5	-120.567666053772000
a_6	60.741998672485400
a_7	-12.725062847137500

b) Battjes and Stive (1985), hereafter referred to as BS85, used the same energy dissipation model as BJ78 (Equation 3). They modified the model of BJ78 by recalibrating the coefficient γ in the breaker height formula (Equation 5). The coefficient γ was related to the deepwater wave steepness (H_{rmso}/L_o) . After calibration with small-scale and

field experiments, the breaker height formula was modified to be:

$$H_b = 0.14L\tanh\left\{\left[0.57+0.45\tanh\left(33\frac{H_{rmso}}{L_o}\right)\right]kh\right\} \quad (7)$$

where H_{rmso} is the deepwater *rms* wave height, and L_o is the deepwater wavelength. Hence, the main difference between the models of BJ78 and BS85 is only the formula for computing H_b.

c) Baldock *et al.* (1998), hereafter referred to as BHV98, proposed to compute D_B by integrating from H_b to ∞ the product of the dissipation for a single broken wave and the *pdf* of the wave heights. The energy dissipation of a single broken wave is described by the bore model of BJ78. The *pdf* of wave heights inside the surf zone was assumed to be a Rayleigh distribution. The result is:

$$D_B = \begin{cases} \exp\left[-\left(\frac{H_b}{H_{rms}}\right)^2\right]\frac{\rho g\left(H_b^2+H_{rms}^2\right)}{4T_p} & for \quad H_{rms} < H_b \\ \exp[-1]\frac{2\rho g H_b^2}{4T_p} & for \quad H_{rms} \geq H_b \end{cases} \quad (8)$$

in which the breaker height (H_b) is determined from the formula of Nairn (1990) as:

$$H_b = h\left[0.39+0.56\tanh\left(33\frac{H_{rmso}}{L_o}\right)\right] \quad (9)$$

Although the model of BHV98 (Equation 8) seems to be quite different from the D_B model of BJ78, it can be rewritten in the similar form as that of BJ78 as:

$$D_B = Q_{b2}\frac{\rho g H_b^2}{4T_p} \quad (10)$$

in which Q_{b2} is a function of H_{rms}/H_b as:

$$Q_{b2} = \begin{cases} \left[1+\left(\frac{H_{rms}}{H_b}\right)^2\right]\exp\left[-\left(\frac{H_{rms}}{H_b}\right)^{-2}\right] & for \quad \frac{H_{rms}}{H_b} < 1 \\ 2\exp[-1] & for \quad \frac{H_{rms}}{H_b} \geq 1 \end{cases} \quad (11)$$

Comparing with the model of BJ78, the parameter Q_{b2} may be also considered as the fraction of breaking waves. The main difference between the models of BJ78 and BHV98 are the formulas for computing H_b and Q_b.

d) Ruessink *et al.* (2003), hereafter referred to as RWS03, used the same energy dissipation model as BHV98 (Equation 8), but a different breaker height formula. The breaker height formula of BJ78 (Equation 5) is modified by adding the term kh into the formula. After calibration with field experiments, the breaker height formula was modified to be:

$$H_b = 0.14L\tanh[(0.86kh+0.33)kh] \quad (12)$$

3. Model Development

In this study, the energy dissipation model of BJ78 is used as a framework for developing the present energy dissipation model. Similar to the model of BJ78, the present model is expressed as:

$$D_B = Q_{b3}\frac{\rho g H_b^2}{4T_p} \quad (13)$$

where Q_{b3} is the fraction of breaking waves of the present study, which is a function of H_{rms}/H_b.

It can be seen from Section 2 that the main difference among the existing models are the formulas for computing Q_b and H_b. It is not clear, which formulas of H_b and Q_b are suitable for modeling D_B (or computing H_{rms}). The objective of this section is to determine suitable formulas of H_b and Q_b for computing the *rms* wave height transformation.

The model of BJ78 was derived based on two main assumptions, the assumptions of truncated-Rayleigh distribution of wave heights and a simplified bore-type dissipation model. It should be noted that the assumption of a truncated-Rayleigh distribution, which is used to derive the formula of Q_b, is not supported by laboratory and field data (Dally, 1990). Some researchers (e.g. Southgate and Nairn, 1993; and Baldock *et al.*, 1998) demonstrated that Equation 4 gives a large error in predicting the fraction of breaking waves (Q_b). Moreover, the simplified bore-type dissipation model for estimating energy dissipation of a single breaking wave ($D_{BS} = \rho g H^2/4T$) is also not supported by laboratory data (Rattanapitikon *et al.*, 2003). Surprisingly, the D_B model of BJ78 seems to give good results in predicting H_{rms} and has proven to be a popular framework for estimating H_{rms} (Ruessink *et al.*, 2003). Because the assumptions for deriving the model are not valid, but the model gives good results in predicting H_{rms}, the D_B model of BJ78 may be considered as an empirical model for computing only H_{rms} (not for computing Q_b and a single breaking wave). As the model is an empirical model, it may not be necessary to derive the formula of Q_b by assuming the *pdf* of wave heights inside the surf zone (as done by BJ78 and BHV98). Moreover, the acceptable *pdf* of wave heights inside the surf zone is not available (Demerbilek and Vincent, 2006). It may not be suitable to derive formulas of Q_b from the assumed *pdf* of wave heights. Alternatively, the formula of Q_b can be derived directly from the measured wave heights by inverting the energy dissipation model (Equation 13) and the wave model (Equation 2). Therefore, in the present study, the formula of Q_b will be newly derived from the measured wave heights.

As Q_b is the function of H_{rms}/H_b, the formula of Q_b can be determined by plotting a relationship between measured Q_b versus H_{rms}/H_b. The required data for determining the formula are the measured data of Q_b and H_{rms}/H_b. The measured Q_b can be determined from the measured wave heights as the following.

Substituting Equation 2 into Equation 13 and using

a backward finite difference scheme to describe the differential equation, the variable Q_{b3} is expressed as:

$$Q_{b3i} = \frac{T_p}{2H_b^2} \frac{\left(H_{rmsi-1}^2 c_{gi-1} \cos\theta_{i-1} - H_{rmsi}^2 c_{gi} \cos\theta_i\right)}{x_i - x_{i-1}} \quad (14)$$

where i is the grid number and the originate of i is at the offshore boundary. Hereafter, the variable Q_{b3} determined from Equation 14 is referred to as measured Q_{b3}.

For determining Q_{b3} from Equation 14, a formula of H_b must be given. As there are four existing breaker height formulas (Equations. 5, 7, 9, and 12), four Q_{b3} can be determined and consequently four relationships between measured Q_{b3} and H_{rms}/H_b are considered in this study. The required data set for determining the measured Q_{b3} are the measured values of h, T_p, H_{rms}, θ, and x. Other related variables (e.g. H_{rmso}, L_o, L, k, and c_g) are computed based on linear wave theory. To avoid a large fluctuation in the relationships, the wave heights variation across the shore should have a small fluctuation.

Because of a variety of wave conditions and a small fluctuation of wave heights variation across the shore, the data from Dette *et al.* (1998) are used for deriving the formulas of Q_{b3} for H_b the four formulas. An example of measured wave height transformation across-shore is shown in Figure 1. However, all collected data shown in Table 1 are used for verification of the models.

The four relationships between measured Q_{b3} versus H_{rms}/H_b (using Equations 5, 7, 9, and 12 for computing H_b) have been plotted to determine a suitable formula of Q_{b3} (see Figures 2 to 5). It can be seen from Figures 2 to 5 that all relationships are fitted well with a quadratic equation as:

$$Q_{b3} = C_1 + C_2\left(\frac{H_{rms}}{H_b}\right) + C_3\left(\frac{H_{rms}}{H_b}\right)^2 \text{ for } \frac{H_{rms}}{H_b} > C_4 \quad (15)$$

where C_1 to C_4 are constants. The fraction of breaking waves

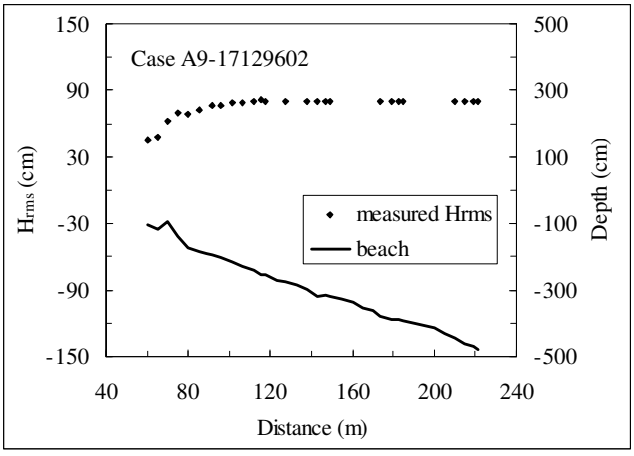

Figure 1. Example of measured wave height transformation across-shore (measured data from Dette *et al.'*, 1998, case A9-17129602).

(Q_{b3}) is set to be zero when $H_{rms}/H_b \le C_4$ (in the offshore zone). The constants C_1 to C_3 can be determined by fitting the curves in Figures 2 to 5. As the constant C_4 is the point where Q_{b3}= 0 (x-intercept), it can be determined from the known constants C_1 to C_3 by solving the quadratic equation. The constants C_1 to C_4 and correlation coefficients (R^2) of

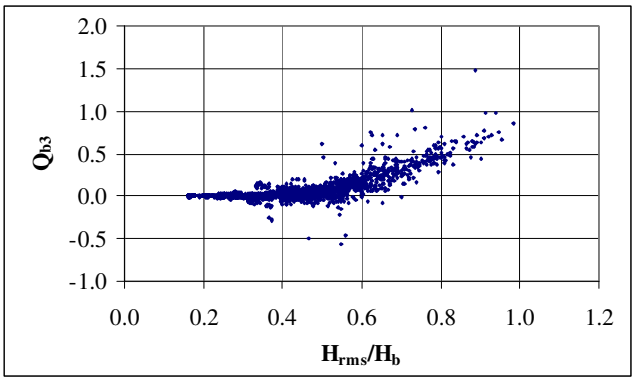

Figure 2. Relationship between measured Q_{b3} versus H_{rms}/H_b in which Equation 5 is used for computing H_b (measured data from Dette *et al.*, 1998).

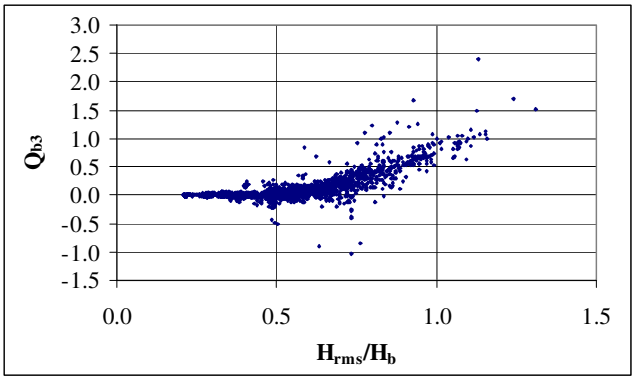

Figure 3. Relationship between measured Q_{b3} versus H_{rms}/H_b in which Equation 7 is used for computing H_b (measured data from Dette *et al.*, 1998).

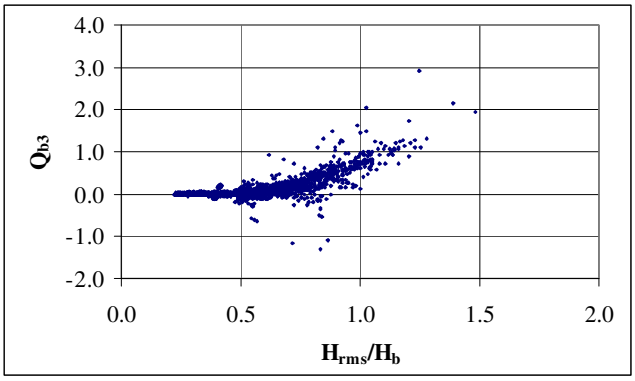

Figure 4. Relationship between measured Q_{b3} versus H_{rms}/H_b in which Equation 9 is used for computing H_b (measured data from Dette *et al.*, 1998).

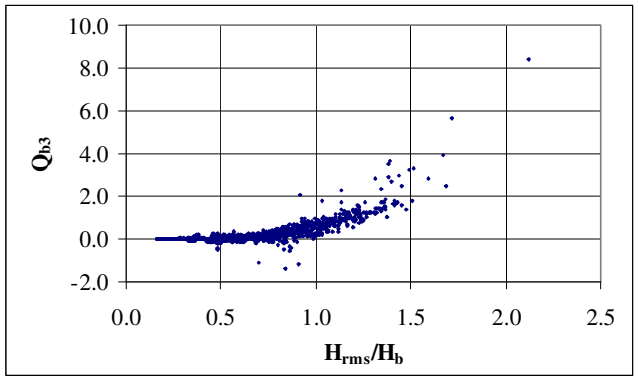

Figure 5. Relationship between measured Q_{b3} versus H_{rms}/H_b in which Equation 12 is used for computing H_b (measured data from Dette *et al.*, 1998).

Equation 15 for four H_b formulas are shown in Table 3. The correlation coefficients (R^2) of the fitting vary between 0.73 to 0.83, which indicates a reasonably good fit.

It should be noted that an attempt is also made to fit the measured Q_{b3} with a cubic equation. However, it is found that the correlation coefficients (R^2) of all models did not significantly improve. Therefore, the quadratic equation is used in this study.

Substituting the formula of for each H_b formula Q_{b3} into Equation 13, the present D_B models (MD1-MD4) can be expressed as:

MD1:

$$D_B = \frac{\rho g H_b^2}{4T}\left[0.189 - 1.282\left(\frac{H_{rms}}{H_b}\right) + 2.073\left(\frac{H_{rms}}{H_b}\right)^2\right]$$

$$\text{for } \frac{H_{rms}}{H_b} > 0.37 \qquad (16)$$

in which H_b is determined from the breaker height formula of BJ78 (Equation 5).

MD2:

$$D_B = \frac{\rho g H_b^2}{4T}\left[0.293 - 1.601\left(\frac{H_{rms}}{H_b}\right) + 2.096\left(\frac{H_{rms}}{H_b}\right)^2\right]$$

$$\text{for } \frac{H_{rms}}{H_b} > 0.46 \qquad (17)$$

in which H_b is determined from the breaker height formula of BS85 (Equation 7).

MD3:

$$D_B = \frac{\rho g H_b^2}{4T}\left[0.309 - 1.614\left(\frac{H_{rms}}{H_b}\right) + 2.013\left(\frac{H_{rms}}{H_b}\right)^2\right]$$

$$\text{for } \frac{H_{rms}}{H_b} > 0.49 \qquad (18)$$

in which H_b is determined from the breaker height formula of Nairn (1990) (Equation 9).

MD4:

$$D_B = \frac{\rho g H_b^2}{4T}\left[0.342 - 1.776\left(\frac{H_{rms}}{H_b}\right) + 2.087\left(\frac{H_{rms}}{H_b}\right)^2\right]$$

$$\text{for } \frac{H_{rms}}{H_b} > 0.56 \qquad (19)$$

in which H_b is determined from the breaker height formula of RWS03 (Equation 12).

4. Model Examination

In the beach morphodynamics model, the wave model has to be run several times to account for the change of beach morphology. It is necessary to estimate the wave height with a high accuracy, because the error of the estimation may be accumulate over time. The objective of this section is to examine the applicability of the present dissipation models on simulating *rms* wave heights (H_{rms}) and to select the best one. To confirm the ability of the present models, the accuracy of the present models was also compared with that of four existing models (shown in Section 2). The measured *rms* wave heights from 13 sources (1723 cases) of collected experimental results (shown in Table 1) are used to examine the models. The collected data are separated into three groups according to the experiment scales, i.e. small-scale, large-scale, and field experiments. It is expected that a good model should be able to predict well for the three groups of experimental scales and well for all collected data.

The basic parameter for determination of the accuracy of a model is the average relative error (*ER*), which is defined as:

Table 3. Calibrated constants (C_1 to C_4) and correlation coefficients (R^2) of Q_{b3} formula (Equation 15) for the four H_b formulas.

No.	Q_{b3} Formulas	H_b Formulas	Calibrated constants				R^2
			C_1	C_2	C_3	C_4	
1	Eq. (15)	Eq. (5)	0.189	-1.282	2.073	0.37	0.77
2	Eq. (15)	Eq. (7)	0.293	-1.601	2.096	0.46	0.75
3	Eq. (15)	Eq. (9)	0.309	-1.614	2.013	0.49	0.73
4	Eq. (15)	Eq. (12)	0.342	-1.776	2.087	0.56	0.83

Table 4. The average relative errors (*ER*) of the existing and the present models for 3 experiment scales and all collected data (measured data from Table 1).

Models	D_B Formulas	h_b Formulas	*ER*			
			Small-scale (152 data)	Large-scale (6705 data)	Field (11285 data)	All data (18142 data)
BJ78	Eq. (3)	Eq. (5)	8.80	10.05	18.68	15.41
BS85	Eq. (3)	Eq. (7)	6.98	6.68	10.69	9.18
BHV98	Eq. (8)	Eq. (9)	9.93	6.72	11.47	9.70
RWS03	Eq. (8)	Eq. (12)	11.65	8.06	10.73	9.75
MD1	Eq. (16)	Eq. (5)	24.06	8.17	11.56	10.41
MD2	Eq. (17)	Eq. (7)	6.96	6.62	9.77	8.58
MD3	Eq. (18)	Eq. (9)	9.24	7.70	10.24	9.29
MD4	Eq. (19)	Eq. (12)	9.93	9.08	10.94	10.24

$$ER = \frac{100}{N}\sum_{j=1}^{N}\left(\frac{\left|H_{mj} - H_{cj}\right|}{H_{mj}}\right) \qquad (20)$$

where j is the wave height number, H_{cj} is the computed wave height of number j, H_{mj} is the measured wave height of number j, and N is the total number of data of measured wave heights. A small value of *ER* indicates a high level of accuracy of the model.

The *rms* wave height transformation is computed by numerical integration of the energy flux balance equation (Equation 2) with the energy dissipation rate of the existing and the present models (i.e. the models of BJ78, BS85, BHV98, RWS03, and MD1 to MD4). A backward finite difference scheme is used to solve the energy flux balance equation (Equation 2). The *ER* of each dissipation model for three experimental scales and all collected data have been computed and shown in Table 4. The results can be summarized as follows:

a) The *ER* of the models for small-scale experiments varies between 7.0% and 24.1%. The accuracy of the models for small-scale experiments in descending order are MD2, BS85, BJ78, MD3, BHV98, MD4, RWS03, and MD1.

b) The *ER* of the models for large-scale experiments varies between 6.6% and 10.1%. The accuracy of the models for large-scale experiments in descending order are MD2, BS85, BHV98, MD3, RWS03, MD1, MD4, and BJ78.

c) The *ER* of the models for field experiments varies between 9.8% and 18.7%. The accuracy of the models for field experiments in descending order are MD2, MD3, BS85, RWS03, MD4, BHV98, MD1, and BJ78.

d) The of the models for all collected data, which is used to indicate the overall accuracy, varies between 8.6% and 15.4%. The overall accuracy of the models for all collected data in descending order are MD2, BS85, MD3, BHV98, RWS03, MD4, MD1, and BJ78.

e) Comparing the overall accuracy of the existing models (BJ78, BS85, BHV98, and RWS03), the model of BS85 gives the best prediction.

f) Comparing the overall accuracy of the present models (MD1-MD4), the model of MD2 gives the best prediction.

g) Considering the overall performance of all models, the model MD2 seems to be the best one. Therefore, MD2 is recommended to use for computing the transformation of H_{rms}.

It can be seen that the model MD2 is similar to the model of BS85. The main difference between the models MD2 and BS85 is the formula of Q_b which makes the model MD2 simpler than the model BS85. Although the model MD2 is simpler than BS85, the accuracy is better.

5. Conclusions

A simple energy dissipation model for computing the *rms* wave height transformation was developed. The *rms* wave height transformation is computed from the energy flux conservation law. The dissipation model of Battjes and Janssen (1978) was used as a framework for developing the present model. The model of Battjes and Janssen (1978) consists of three main formulas, (a) the formulas of energy dissipation of a single broken wave, (b) the breaker height (H_b), and (c) the fraction of breaking waves (Q_b). The present study focuses mainly on the new derivation of the Q_b formula. Unlike the common derivation, the formula of Q_b was derived directly from the measured wave heights by inverting the wave model together with the dissipation model. Based on the four existing breaker height formulas, four Q_b formulas were developed and consequently yielded four dissipation models.

A wide range and large amount of collected experimental data (1723 cases collected from 13 sources) were used to examine the applicability of the present dissipation models on simulating H_{rms} and to select the best one. To confirm the ability of the proposed models, their accuracy was also compared with that of four existing dissipation models. The examination results were presented in terms of average relative error. The examination shows that the model

MD2 gives very good accuracy for a wide range of wave and beach conditions (with *ER* for all collected data of 8.6%) and gives better predictions than that of existing models.

Acknowledgements

This research was sponsored by the Thailand Research Fund and the Commission on Higher Education, Ministry of Education, Thailand. The data collection of the DELILAH and DUCK94 Projects were funded by the US Office of Naval Research and the US National Science Foundation, U.S.A.

References

Baldock, T.E., Holmes, P., Bunker, S. and Van Weert, P. 1998. Cross-shore hydrodynamics within an unsaturated surf zone. Coastal Engineering. 34, 173-196.

Battjes, J.A. and Janssen, J.P.F.M. 1978. Energy loss and set-up due to breaking of random waves. Proceedings of the 16th Coastal Engineering Conference, American Society of Civil Engineers, 569-587.

Battjes, J.A. and Stive, M.J.F. 1985. Calibration and verification of a dissipation model for random breaking waves. Journal of Geophysical Research. 90, 9159-9167.

Birkemeier, W.A., Donoghue, C., Long, C.E., Hathaway, K.K. and Baron, C.F. 1997. The DELILAH Nearshore Experiment: Summary Data Report. US Army Corps of Engineers, Waterways Experiment Station, Vicksburg, MS.

Dally, W. R., Dean, R. G. and Dalrymple, R. A. 1985. Wave height variation across beach. Journal of Geophysical Research. 90(C6), 11917-11927.

Dally, W.R. 1990. Random breaking waves: A closed-form solution for planar beaches. Coastal Engineering. 14, 233-263.

Demerbilek, Z. and Vincent, L. 2006. Water wave mechanics (Part 2 - Chapter 1). Coastal Engineering Manual, EM1110-2-1100, Coastal and Hydraulics Laboratory - Engineering Research and Development Center, Waterways Experiment Station, US Army Corps of Engineers, pp. II-1-75.

Dette, H.H, Peters, K. and Newe, J. 1998. MAST III - SAFE Project: Data Documentation, Large Wave Flume Experiments '96/97. Report No. 825 and 830. Leichtweiss-Institute, Technical University Braunschweig.

Grasmeijer, B.T. and van Rijn, L.C. 1999. Transport of fine sands by currents and waves, III: breaking waves over barred profile with ripples. Journal of Waterways, Port, Coastal, and Ocean Engineering, American Society of Civil Engineers. 125, 71-79.

Hamilton, D.G. and Ebersole, B.A. 2001. Establishing uniform longshore currents in a large-scale sediment transport facility. Coastal Engineering. 42, 199-218.

Herbers, T.H.C., Elgar, S., Guza, R.T. and O'Reilly, W.C. 2006. Surface gravity waves and nearshore circulation. DUCK94 Experiment Data Server: SPUV Pressure Sensor Wave Height Data. Available online at: http://dksrv.usace.army.mi/jg/dk94dir [April 7, 2006].

Horikawa, K. and Kuo, C. T. 1966. A study of wave transformation inside the surf zone. Proceedings of the 10th Coastal Engineering Conference, American Society of Civil Engineers, 217-233.

Hurue, M. 1990. Two-Dimensional Distribution of Undertow due to Irregular Waves. B.Eng. Thesis. Department of Civil Engineering, Yokohama National University, Japan (in Japanese).

Johnson, H.K. 2006. Wave modelling in the vicinity of submerged breakwaters. Coastal Engineering. 53, 39-48.

Kraus, N.C., Gingerich, K.J. and Rosati, J.D. 1989. DUCK85 Surf Zone Sand Transport Experiment. Technical Report CERC-89-5. US Army Corps of Engineers, Waterways Experiment Station, Vicksburg, MS.

Kraus, N.C. and Smith, J.M. 1994. SUPERTANK Laboratory Data Collection Project. Technical Report CERC-94-3. US Army Corps of Engineers, Waterways Experiment Station, Vicksburg, MS.

Le Mehaute, B. 1962. On non-saturated breakers and the wave run-up. Proceedings of the 8th Coastal Engineering Conference, American Society of Civil Engineers, 77-92.

Mizuguchi, M. 1981. An heuristic model of wave height distribution in surf zone. Proceedings of the 17th Coastal Engineering Conference, American Society of Civil Engineers, 278-289.

Miche, R. 1951. Le pouvoir reflechissant des ouvrages maritime exposes a l'action de la houle. Annales Ponts et Chaussees, 121 Annee, pp. 285-319.

Nairn, R.B. 1990. Prediction of Cross-Shore Sediment Transport and Beach Profile Evolution. Ph.D. thesis, Department of Civil Engineering, Imperial College, London.

Oliveira, F.S.B.F. 2007. Numerical modeling of deformation of multi-directional random wave over a varying topography. Ocean Engineering. 34, 337-342.

Rattanapitikon, W. and Shibayama T. 1998. Energy dissipation model for regular and irregular breaking waves. Coastal Engineering Journal, Japan Society of Civil Engineers. 40, 327-346.

Rattanapitikon, W. and Leangruxa, P. 2001. Comparison of dissipation models for regular breaking waves. Songklanakarin Journal of Science and Technology. 23, 63-72.

Rattanapitikon, W., Karunchintadit, R. and Shibayama, T. 2003. Irregular wave height transformation using representative wave approach. Coastal Engineering Journal, Japan Society of Civil Engineers. 45, 489-510.

Roelvink, J.A. and Reniers A.J.H.M. 1995. LIP 11D Delta Flume Experiments: A Data Set for Profile Model Validation. Report No. H 2130. Delft Hydraulics.

Ruessink, B.G., Walstra, D.J.R. and Southgate, H.N. 2003. Calibration and verification of a parametric wave

model on barred beaches. Coastal Engineering. 48, 139-149.

Sawaragi, T. and Iwata, K. 1974. Turbulence effect on wave deformation after breaking. Coastal Engineering in Japan, Japan Society of Civil Engineers. 17, 39-49.

Smith, J.M. and Kraus, N.C. 1990. Laboratory Study on Macro-Features of Wave Breaking Over Bars and Artificial Reefs. Technical Report CERC-90-12. US Army Corps of Engineers, Waterways Experiment Station, Vicksburg, MS.

Southgate, H.N. and Nairn, R.B. 1993. Deterministic profile modelling of nearshore processes, Part 1: Waves and currents. Coastal Engineering. 19, 27-56.

Sultan, N. 1995. Irregular Wave Kinematics in the Surf Zone. Ph.D. Dissertation. Texas A&M University, College Station, Texas, USA.

Thornton, E.B. and Guza, R.T. 1986. Surf zone longshore currents and random waves: field data and model. Journal of Physical Oceanography. 16, 1165-1178.

Ting, F.C.K. 2001. Laboratory study of wave and turbulence velocity in broad-banded irregular wave surf zone. Coastal Engineering. 43, 183-208.

A.6 Modification of a parametric model

Reprinted from:

Rattanapitikon, W. and Sawanggun, S. (2007). Modification of a parametric model, The 4th International Conference on Asian and Pacific Coasts [CD-ROM], September 21-24, Nanjing, China, pp. 346-357.

Asian and Pacific Coasts 2007
September 21-24, 2007, Nanjing, China

MODIFICATION OF A PARAMETRIC WAVE MODEL

Winyu Rattanapitikon[1] and Sangapol Sawanggun[2]

ABSTRACT: This study was undertaken to develop a simple wave model for computing the transformation of root mean square wave height. The parametric wave approach of Battjes and Janssen (1978) was used as a framework for developing the models. The energy dissipation in the wave model is expressed as the product of fraction of breaking waves and energy dissipation of a single broken wave. The fraction of breaking waves was modified in this study. The fraction of breaking waves was not derived from the assumed probability of wave breaking (as did in the common derivation), but derived directly from the measured wave heights by inverting the wave model. Experimental data of root mean square wave height transformation from 13 sources, covering 1,723 cases of wave and beach conditions, have been collected for verifying the models. The experiments cover a wide range of wave and beach conditions, including small-scale, large-scale and field experiments. The modified model was also compared with three existing models, which were developed based on the parametric wave approach. The modified model gives very good accuracy for a wide range of wave and beach conditions and better than those of existing models.

1. Introduction

Wave height is one of the most essential required factors for many coastal engineering applications such as the design of coastal structures and the study of beach deformations. When waves propagate in shallow water, their profiles steepen and they eventually break. The higher waves tend to break at a greater distance from the shore. Closer to the shore, more and more waves break, until almost all the waves break in the inner surf zone. Once the waves start to break, a part of the wave energy is transformed into turbulence and heat, and wave height decreases towards the shore. Common methods to model irregular wave height transformation can be classified into four main approaches, i.e. representative wave approach, spectral approach, probabilistic approach, and parametric wave approach. For computing beach deformation, the wave model should be kept as simple as possible because of the frequent updating of wave fields to account for the change of bottom profiles. The parametric and representative wave approaches appear to be simple methods and seem to be suitable for incorporating in the beach deformation model.

[1] Associate Professor, Civil Engineering Program, Sirindhorn International Institute of Technology, Thammasat University, Pathum Thani 12121, Thailand. winyu@siit.tu.ac.th
[2] Graduate student, ditto

For the representative wave approach, the regular wave model has been directly applied to irregular waves by using representative (or equivalent) waves, while the parametric approach considers the random nature of the waves but describes the energy dissipation rate in terms of time-averaged parameters. The parametric wave models were developed based on the assumed probability density function (*pdf*) of wave height inside the surf zone. The average rate of energy dissipation is described by integrating the product of energy dissipation of a broken wave and the probability of occurrence of breaking waves. The parametric wave approach is expected to be better than the representative wave approach because it includes the random nature of the waves into the model while the other does not. Therefore, the present study focuses on the parametric wave approach.

The parametric wave models are generally based on the work of Battjes and Janssen (1978). The model relies on the macroscopic features of breaking waves and predicts only the transformation of root-mean-square (*rms*) wave height. The *rms* wave height transformation is computed from the energy flux conservation law. It is

$$\frac{\partial\left(Ec_g\cos\theta\right)}{\partial x} = -D_B \tag{1}$$

where E is the wave energy density, c_g is the group velocity, θ is the mean wave angle, x is the distance in the cross shore direction, and D_B is the energy dissipation rate due to wave breaking. The energy dissipation rate due to bottom friction is neglected. All variables are based on linear wave theory and Snell's law is employed to describe wave refraction.

From linear wave theory, the wave energy density (E) is equal to $\rho g H_{rms}^2/8$. Therefore, Eq. (1) can be written in terms of wave height as

$$\frac{\rho g}{8}\frac{\partial\left(H_{rms}^2 c_g\cos\theta\right)}{\partial x} = -D_B \tag{2}$$

where ρ is the density of water, g is the gravity acceleration, and H_{rms} is the *rms* wave height.

The *rms* wave height transformation can be computed from the energy flux balance equation [Eq. (2)] by substituting the model of energy dissipation rate (D_B) and numerically integrating from offshore to shoreline. In the offshore zone, the energy dissipation rate is set to zero. The main difficulty of Eq. (2) is how to formulate the energy dissipation rate caused by the breaking waves.

During the past decades, various energy dissipation models for the parametric wave approach have been proposed for computing H_{rms} in the surf zone. Because of the complexity of the wave breaking mechanism, most of the energy dissipation models were developed based on an empirical or semi-empirical approach. It is well known that the validity of an empirical formula may be limited according to the range of experimental conditions that were employed in the calibrations or verifications. To make an empirical formula reliable, it is necessary to calibrate or verify the formula with a large amount and wide range of experimental data. Since many energy dissipation models were developed based on data with limited experimental conditions, there is still a need for more data to confirm the underlying assumptions and to make the model more reliable. It is the purpose of this study to develop a simple energy dissipation model for the parametric wave approach based on a wide range of experimental conditions.

Experimental data of *rms* wave height transformation from 13 sources, covering 1,723 cases of wave and beach conditions, have been collected for verifying the models. The experiments cover a wide range of wave and beach conditions, including small-scale, large-scale and field experiments. The experiments cover a variety of beach conditions (i.e. plane, barred, and sandy beaches) and a range of deepwater wave steepness (H_{rmso}/L_o) from 0.001 to 0.059. A summary of the collected experimental data is given in Table 1.

Table 1 Summary of collected experimental data

Sources	**Total no. of cases**	**Total no. of data**	**Beach conditions**	H_{rmso}/L_o	**Apparatus**
Hurue (1990)	1	7	plane beach	0.026	small-scale
Smith and Kraus (1990)	12	96	plane and barred beach	0.021-0.059	small-scale
Sultan (1995)	1	12	plane beach	0.004	small-scale
Grasmeijer and Rijn (1999)	2	20	sandy beach	0.014-0.017	small-scale
Hamilton and Ebersole (2001)	1	10	plane beach	0.017	small-scale
Ting (2001)	1	7	plane beach	0.016	small-scale
Kraus and Smith (1994): SUPERTANK project	128	2,223	sandy beach	0.001-0.045	large-scale
Roelvink and Reniers (1995): LIP 11D project	95	923	sandy beach	0.004-0.028	large-scale
Dette et al. (1998): MAST III – SAFE project	138	3,559	sandy beach	0.006-0.015	large-scale
Thornton and Guza (1986)	4	60	sandy beach	0.001-0.001	field
Kraus et al. (1989): DUCK85 project	8	90	sandy beach	0.001-0.002	field
Birkemeier et al. (1997): DELILAH project	745	5,033	sandy beach	0.001-0.025	field
Herbers et al. (2006): DUCK94 project	587	6,102	sandy beach	0.001-0.029	field
Total	1,723	18,142		0.001-0.059	

This paper is divided into three main parts. The first part briefly reviews some existing dissipation models for the parametric wave approach. The second part describes the development of the present model. The last part is the verification of the present model in comparison with the existing models.

2. Existing Energy Dissipation Models

During the past decades, various energy dissipation models have been developed based on a framework of the parametric wave approach of Battjes and Janssen (1978). Brief reviews of some existing dissipation models are described below.

a) Battjes and Janssen (1978), hereafter referred to as BJ78, proposed to compute D_B as a product of the fraction of breaking waves (Q_b) and the energy dissipation of a single broken wave (D_s) as

$$D_B = Q_{b1} D_{s1} \tag{3}$$

where Q_{b1} is the fraction of breaking waves of BJ78, and D_{s1} is the energy dissipation of a single broken wave (or a possible maximum wave height) of BJ78. The energy dissipation of a single broken wave is determined from a simplified bore-type dissipation model as

$$D_{s1} = \frac{\rho g H_b^2}{4T_p} \tag{4}$$

where H_b is the breaker height or the maximum wave height, and T_p is the spectral peak period. The fraction of breaking waves (Q_{b1}) was derived based on the assumption that the probability density function (*pdf*) of wave height could be modeled with a Rayleigh distribution truncated at the breaker height (H_b) and all broken waves have a height equal to the breaker height (H_b). This was shown to imply the relation between Q_{b1} and H_{rms}/H_b as

$$\frac{1 - Q_{b1}}{-\ln Q_{b1}} = \left(\frac{H_{rms}}{H_b} \right)^2 \tag{5}$$

in which the breaker height (H_b) is determined from the formula of Miche (1951) with an additional coefficient (γ) in the tan-hyperbolic function as

$$H_b = 0.14 L \tanh(\gamma k h) \tag{6}$$

where L is the wavelength related to T_p, k is the wave number, and h is the water depth. Based on their small-scale experimental data, the coefficient γ is determined to be 0.91. As Eq. (5) is an implicit equation, it has to be solved for Q_{b1} by an iteration technique, or by a 1-D look-up table (Southgate and Nairn, 1993), or by fitting Q_{b1} with a polynomial function as

$$Q_{b1} = \sum_{n=0}^{7} a_n \left(\frac{H_{rms}}{H_b} \right)^n \tag{7}$$

where a_n is the constant of n^{th} term. A multiple regression analysis is used to determine the constants a_o to a_7. The correlation coefficient (R^2) of Eq. (7) is 0.99999999. The values of constants a_o to a_7 are shown in Table 2. Equation (7) is applicable for $0.3 < H_{rms}/H_b < 1.0$. For $H_{rms}/H_b \leq 0.3$, the value of Q_{b1} is very small and can be set at zero. The value of Q_{b1} is set to be 1.0 when $H_{rms}/H_b \geq 1.0$. The model of BJ78 has been used successfully in many applications for computing H_{rms} transformation (e.g. Abadie et al., 2006; Johnson, 2006; and Oliveira, 2007). The D_B model of BJ78 was derived based on two main assumptions, i.e. assumptions of the truncated-Rayleigh distribution of wave height and the simplified bore-type dissipation model. It should be noted that the assumption of the truncated-Rayleigh distribution (for deriving the

formula of Q_{b1}) is not supported by experimental data (Dally, 1990). Some researchers (e.g. Southgate and Nairn, 1993; and Baldock et al., 1998) demonstrated that Eq. (5) gives a large error in predicting the fraction of breaking waves (Q_b). Moreover, the simplified bore-type dissipation model for estimating energy dissipation of a broken wave is also not supported by experimental data (Rattanapitikon et al., 2003). Surprisingly, the D_B model of BJ78 seems to give good results of predicting H_{rms} and has proven to be a popular framework for estimating H_{rms} (Ruessink et al., 2003). Because the assumptions for deriving the model are not valid but the model still gives very good results, the D_B model of BJ78 may be considered as an empirical model for computing only D_B or H_{rms}.

Table 2 Values of constants a_o to a_7 for computing Q_{b1}

Constants	Values
a_0	0.2317072
a_1	-3.6095814
a_2	22.5948312
a_3	-72.5367918
a_4	126.8704405
a_5	-120.5676384
a_6	60.7419815
a_7	-12.7250603

b) Battjes and Stive (1985), hereafter referred to as BS85, used the same energy dissipation model as that of BJ78 [Eq. (3)]. They modified the model of BJ78 by recalibrating the coefficient γ in the breaker height formula [Eq. (6)]. The coefficient γ was related to the deepwater wave steepness (H_{rmso}/L_o). After calibration with small-scale and field experiments, the breaker height formula was modified to be

$$H_b = 0.14L\tanh\left\{\left[0.57 + 0.45\tanh\left(33\frac{H_{rmso}}{L_o}\right)\right]kh\right\} \tag{8}$$

where H_{rmso} is the deepwater *rms* wave height, and L_o is the deepwater wavelength. Hence, the main difference between the models of BJ78 and BS85 is only the formula for computing H_b.

c) Southgate and Nairn (1993), hereafter referred to as SN93, modified the model of BJ78 by changing the expression of energy dissipation of a single broken wave from the bore model of BJ78 (D_{s1}) to be the bore model of Thornton and Guza (1983), D_{s2}, as

$$D_B = Q_{b1}D_{s2} \tag{9}$$

in which Q_{b1} is the fraction of breaking waves of BJ78 [Eq. (5)] and D_{s2} is the energy dissipation of a single broken wave of Thornton and Guza (1983), which is expressed as

$$D_{s2} = \frac{\rho g H_b^3}{4 T_p h} \tag{10}$$

The breaker height (H_b) is determined from the formula of Nairn (1990) as

$$H_b = h\left[0.39 + 0.56 \tanh\left(33 \frac{H_{rmso}}{L_o}\right)\right] \tag{11}$$

Hence, the model of SN93 is similar to that of BJ78 except for the formulas of D_{s2} and H_b.

3. Model Development

In this study, the energy dissipation model of BJ78 is used as a framework for developing the present energy dissipation model. The D_B model is expressed as the product of fraction of breaking waves (Q_b) and energy dissipation of a single broken wave (D_s).

$$D_B = Q_b D_s \tag{12}$$

in which Q_b is a function of H_{rms}/H_b.

Since the energy dissipation of a single broken wave (D_s) is the energy dissipation of a possible maximum wave height, it may be considered as a maximum energy dissipation or a potential energy dissipation. The fraction of breaking waves (Q_b) may also be considered as a fraction of energy dissipation. The dissipation models [Eq. (12)] may be re-explained as a product of a fraction of energy dissipation and the potential energy dissipation.

The model of D_B consists of 3 main formulas, i.e. the formulas of H_b, Q_b, and D_s. The Q_b formula of BJ78 was derived based on the assumed *pdf* of wave height in the surf zone, which is not supported by the experimental data (Dally, 1990). Since the acceptable *pdf* of wave height inside the surf zone is not available (Demerbilek and Vincent, 2006), it may not be suitable to derive formula of Q_b from the assumed *pdf* of wave height. Alternatively, the formula of Q_b can be derived directly from the measured wave heights by inverting the energy dissipation model [Eq. (12)] and the wave model [Eq. (2)]. Therefore, in the present study, the formula of Q_b will be newly derived from the measured wave heights.

As Q_b is the function of H_{rms}/H_b, the formula of Q_b can be determined by plotting a relationship between measured Q_b versus H_{rms}/H_b. The required data for determining the formula are the measured data of Q_b and H_{rms}/H_b. The measured Q_b can be determined indirectly from the measured wave heights as follows.

Substituting Eq. (2) into Eq. (12), and using backward finite difference scheme to describe the differential equation, the formula for determining measured Q_b is expressed as

$$Q_{bi} = \frac{\rho g}{8 D_s} \frac{\left(H_{rmsi-1}^2 c_{gi-1} \cos\theta_{i-1} - H_{rmsi}^2 c_{gi} \cos\theta_i\right)}{x_i - x_{i-1}} \tag{13}$$

where i is the grid number. Hereafter, the variable Q_b determined from Eq. (13) is referred to as the measured Q_b.

For determining Q_b from Eq. (13), the formulas of D_s and H_b must be given. It can be seen from Sec. 2 that several formulas have been proposed for computing H_b and D_s, i.e. three formulas for H_b [Eqs. (6), (8), and (11)] and two formulas for D_s [Eqs. (4), and (10)]. It is not clear which formulas of H_b and D_s are suitable for modeling Q_b. Therefore, all of them are considered in the derivation of Q_b formula. As there are two formulas for D_s [Eqs. (4), and (10)] and three formulas for H_b [Eqs. (6), (8), and (11)], a total of six Q_b can be determined and consequently six relationships between measured Q_b versus H_{rms}/H_b are considered in this study. The required data set for deriving the formula of Q_b are the measured data of h, T, H_{rms}, θ, and x. Other related variables (e.g. H_{rmso}, L_o, L, k, and c_g) are computed based on linear wave theory. To avoid a large fluctuation in the relationships, the wave heights variation across shore should have a small fluctuation.

Because of a variety of wave conditions and a small fluctuation of wave height variation across shore, the data from Dette et al. (1998) are used for deriving the six formulas of Q_b. However, all collected data shown in Table 1 are used to verify the models for identifying the best one.

The six relationships between measured Q_b versus H_{rms}/H_b have been plotted to identify the suitable equation of the relationships. An example of a relationship between measured Q_b versus H_{rms}/H_b by using Eqs. (4) and (6) for computing D_s and H_b are shown in Fig. 1.

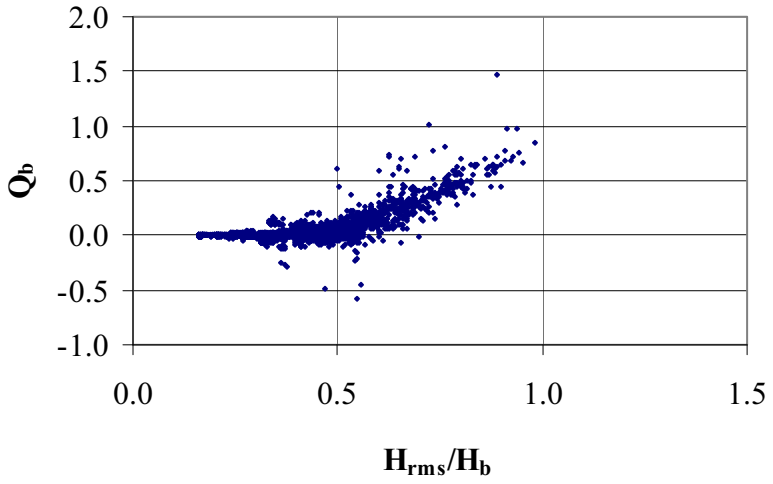

Figure 1 Relationship between measured Q_b versus H_{rms}/H_b by using Eqs. (4) and (6) for computing D_s and H_b (measured data from Dette et al., 1998)

It is found that all relationships can be fitted well with a quadratic equation as

$$Q_b = K_1 + K_2\left(\frac{H_{rms}}{H_b}\right) + K_3\left(\frac{H_{rms}}{H_b}\right)^2 \qquad \text{for} \qquad \frac{H_{rms}}{H_b} > K_4 \tag{14}$$

where K_1 to K_4 are constants. The fraction of energy dissipation (Q_b) is set to be zero when $H_{rms}/H_b \leq K_4$ (offshore zone). The constants K_1 to K_3 can be determined from multi-regression analysis between measured Q_b and H_{rms}/H_b. As the constant K_4 is the point that $Q_b = 0$ (x-intercept), it can be determined from the known constants K_1 to K_3 by solving the quadratic equation. The constants K_1 to K_4 and correlation coefficients (R^2) of the six relationships (6 formulas of Q_b) are shown in Table 3. The correlation coefficients (R^2) of the fitting vary between 0.72 to 0.77, which indicate a reasonably good fit.

Table 3 Calibrated constants (K_1 to K_4) and correlation coefficients (R^2) of Q_b formula [Eq. (14)] for difference D_s and H_b formulas

Formula No.	D_s **Formulas**	H_b **Formulas**	**Calibrated constants**				R^2
			K_1	K_2	K_3	K_4	
F1	Eq. (4)	Eq. (6)	0.189	-1.282	2.073	0.37	0.77
F2		Eq. (8)	0.293	-1.601	2.096	0.46	0.75
F3		Eq. (11)	0.309	-1.614	2.013	0.49	0.73
F4	Eq. (10)	Eq. (6)	0.240	-1.627	2.640	0.37	0.77
F5		Eq. (8)	0.465	-2.532	3.311	0.46	0.74
F6		Eq. (11)	0.544	-2.818	3.485	0.49	0.72

Substituting the six formulas of Q_b into Eq. (12), the six corresponding D_B models (MD1-MD6) can be expressed as

$$\text{MD1: } D_B = \frac{\rho g H_b^2}{4T_p}\left[0.189 - 1.282\left(\frac{H_{rms}}{H_b}\right) + 2.073\left(\frac{H_{rms}}{H_b}\right)^2\right] \qquad \text{for } \frac{H_{rms}}{H_b} > 0.37 \qquad (15)$$

in which H_b is determined from the breaker height formula of BJ78 [Eq. (6)].

$$\text{MD2: } D_B = \frac{\rho g H_b^2}{4T_p}\left[0.293 - 1.601\left(\frac{H_{rms}}{H_b}\right) + 2.096\left(\frac{H_{rms}}{H_b}\right)^2\right] \qquad \text{for } \frac{H_{rms}}{H_b} > 0.46 \qquad (16)$$

in which H_b is determined from the breaker height formula of BS85 [Eq. (8)].

$$\text{MD3: } D_B = \frac{\rho g H_b^2}{4T_p}\left[0.309 - 1.614\left(\frac{H_{rms}}{H_b}\right) + 2.013\left(\frac{H_{rms}}{H_b}\right)^2\right] \qquad \text{for } \frac{H_{rms}}{H_b} > 0.49 \qquad (17)$$

in which H_b is determined from the breaker height formula of Nairn (1990) [Eq. (11)].

$$\text{MD4: } D_B = \frac{\rho g H_b^3}{4T_p h}\left[0.240 - 1.627\left(\frac{H_{rms}}{H_b}\right) + 2.640\left(\frac{H_{rms}}{H_b}\right)^2\right] \qquad \text{for } \frac{H_{rms}}{H_b} > 0.37 \qquad (18)$$

in which H_b is determined from the breaker height formula of BJ78 [Eq. (6)].

$$\text{MD5: } D_B = \frac{\rho g H_b^3}{4 T_p h}\left[0.465 - 2.532\left(\frac{H_{rms}}{H_b}\right) + 3.311\left(\frac{H_{rms}}{H_b}\right)^2\right] \qquad \text{for } \frac{H_{rms}}{H_b} > 0.46 \qquad (19)$$

in which H_b is determined from the breaker height formula of BS85 [Eq. (8)].

$$\text{MD6: } D_B = \frac{\rho g H_b^3}{4 T_p h}\left[0.544 - 2.818\left(\frac{H_{rms}}{H_b}\right) + 3.485\left(\frac{H_{rms}}{H_b}\right)^2\right] \qquad \text{for } \frac{H_{rms}}{H_b} > 0.49 \qquad (20)$$

in which H_b is determined from the breaker height formula of Nairn (1990) [Eq. (11)].

4. Model Examination

In the beach deformation model, the wave model has to be run many times to account for the change of beach profiles. It is necessary to estimate the wave height with high accuracy because the error of the estimation may accumulate from time to time. The objective of this section is to examine the applicability of the present dissipation models (MD1-MD6) on simulating *rms* wave heights and the best one is then selected. To confirm the ability of present models, the accuracy of present models were also compared with that of three existing models (shown in Sec. 2). The measured *rms* wave heights from 13 sources (1,723 cases) of collected experimental results (shown in Table 1) are used to examine the models. The collected experiments are separated into three groups according to the experiment-scales, i.e. small-scale, large-scale, and field experiments. It is expected that a good model should be able to predict well for all experiment-scales and all collected data.

The basic parameter for determination of the accuracy of a model is the average relative error (*ER*), which is defined as

$$ER = \frac{100}{N}\sum_{j=1}^{N}\left(\frac{\left|H_{mj} - H_{cj}\right|}{H_{mj}}\right) \qquad (21)$$

where j is the wave height number, H_{cj} is the computed wave height of number j, H_{mj} is the measured wave height of number j, and N is the total number of data of measured wave heights. The small value of *ER* indicates a high level of accuracy of the model.

The *rms* wave height transformation is computed by numerical integration of the energy flux balance equation [Eq. (2)] with the energy dissipation rate of the existing and the present models [i.e. the models of BJ78, BS85, SN93, and MD1 to MD6]. A backward finite difference scheme is used to solve the energy flux balance equation [Eq. (2)]. The errors (*ER*) of each dissipation model for three experiment-scales and all collected data have been computed and shown in Table 4. The results can be summarized as follows:

a) The error (*ER*) of the models for small-scale experiments varies between 7.0% to 24.1%. The accuracy of the models for small-scale experiments in descending order are MD2, BS85, MD5, BJ78, MD3, MD6, SN93, MD4, and MD1.
b) The error (*ER*) of the models for large-scale experiments varies between 6.6% to 10.1%. The accuracy of the models for large-scale experiments in descending order are MD2, BS85, MD5, MD6, MD3, MD4, MD1, SN93, and BJ78.
c) The error (*ER*) of the models for field experiments varies between 9.8% to 18.7%. The accuracy of the models for field experiments in descending order are MD2, MD3, MD5, BS85, MD6, MD4, MD1, SN93, and BJ78.
d) The error (*ER*) of the models for all collected data, which is used to indicate the overall accuracy, varies between 8.6% to 15.4%. The overall accuracy of the models for all collected data in descending order are MD2, BS85, MD5, MD3, MD6, MD4, MD1, SN93, and BJ78.
e) Comparing the overall accuracy of the existing models (BJ78, BS85, and SN93), the model of BS85 gives the best prediction.
f) Comparing the overall accuracy of the present models (MD1-MD6), the model of MD2 gives the best prediction.
g) Considering the overall performance of all models, the model MD2 seems to be the best. Therefore, the model MD2 is recommended to use for computing the transformation of H_{rms}.

Table 4 Errors (*ER*) of the existing models and the models MD1-MD6 for 3 experiment-scales (measured data from Table 1)

Model	D_B **Formulas**	H_b **Formulas**	**Errors (*ER*)**			
			Small-scale (152 data)	Large-scale (6705 data)	Field (11285 data)	All data (18142 data)
BJ78	Eq. (3)	Eq. (6)	8.80	10.05	18.68	15.41
BS85	Eq. (3)	Eq. (8)	6.98	6.68	10.69	9.18
SN93	Eq. (9)	Eq. (11)	11.61	9.92	15.68	13.52
MD1	Eq. (15)	Eq. (6)	24.06	8.17	11.56	10.41
MD2	Eq. (16)	Eq. (8)	6.96	6.62	9.77	8.58
MD3	Eq. (17)	Eq. (11)	9.24	7.70	10.24	9.29
MD4	Eq. (18)	Eq. (6)	15.70	8.01	11.37	10.16
MD5	Eq. (19)	Eq. (8)	8.76	7.08	10.56	9.26
MD6	Eq. (20)	Eq. (11)	9.30	7.65	10.90	9.69

It can be seen that the model MD2 is similar to the model of BS85. The main difference between the models MD2 and BS85 is the formula of Q_b, which makes the model MD2 simpler than that of BS85. Although the model MD2 is simpler than that of BS85, the accuracy is better.

5. Conclusions

A simple wave model for computing the *rms* wave height transformation was developed. The *rms* wave height transformation is computed from the energy flux conservation. The energy dissipation model of Battjes and Janssen (1978) was used as a framework for developing the

present model. The model of Battjes and Janssen (1978) consists of three main formulas, i.e. the formulas of energy dissipation of a single broken wave (D_s), breaker height (H_b), and fraction of breaking waves (Q_b). The present study focuses mainly on the new derivation of Q_b formula. Unlike the common derivation, the formula of Q_b was derived directly from the measured wave heights by inverting the wave model. Based on the three existing H_b formulas and two existing D_s formulas, six Q_b formulas were developed and consequently yielded six dissipation models.

A wide range and large amount of collected experimental data (1,723 cases collected from 13 sources) were used to examine the applicability of the present models on simulating H_{rms} and select the best one. To confirm the ability of present models, the accuracy of present models were also compared with that of three existing dissipation models. The examination results were presented in terms of average relative error (*ER*). The examination shows that the model MD2 gives very good accuracy for a wide range of wave and beach conditions (with *ER* for all collected data of 8.6%) and gives better predictions than that of existing models. The model MD2 is similar to the model of BS85. The main difference between the models MD2 and BS85 is the formula of Q_b, which makes the model MD2 simpler than that of BS85. Although the model MD2 is simpler than that of BS85, the accuracy is better.

Acknowledgements

This research was sponsored by the Thailand Research Fund. The data collection of the DELILAH and DUCK94 projects were funded by the US Office of Naval Research and the US National Science Foundation.

References

Abadie, S., Butel, R., Mauriet, S., Morichon, D. and Dupuis, H. (2006). Wave climate and longshore drift on the South Aquitaine coast. *Continental Shelf Research,* 26: 1924-1939.

Baldock, T.E., Holmes, P., Bunker, S. and Van Weert, P. (1998). Cross-shore hydrodynamics within an unsaturated surf zone. *Coastal Engineering,* 34: 173-196.

Battjes, J.A. and Janssen, J.P.F.M. (1978). Energy loss and set-up due to breaking of random waves. *Proc. 16th Coastal Engineering Conf., ASCE,* pp. 569-587.

Battjes, J.A. and Stive, M.J.F. (1985). Calibration and verification of a dissipation model for random breaking waves. *J. Geophysical Research,* 90(C5): 9159-9167.

Birkemeier, W.A., Donoghue, C., Long, C.E., Hathaway, K.K. and Baron, C.F. (1997). *The DELILAH Nearshore Experiment: Summary Data Report,* US Army Corps of Engineers, Waterways Experiment Station, Vicksburg, MS.

Dally, W.R. (1990). Random breaking waves: A closed-form solution for planar beaches, *Coastal Engineering,* 14: 233-263.

Demerbilek, Z. and Vincent, L. (2006). Water wave mechanics (Part 2 – Chapter 1). *Coastal Engineering Manual,* EM1110-2-1100, Coastal and Hydraulics Laboratory – Engineering Research and Development Center, WES, US Army Corps of Engineers, pp. II-1-75.

Dette, H.H, Peters, K. and Newe, J. (1998). *MAST III – SAFE Project: Data Documentation, Large Wave Flume Experiments '96/97,* Report No. 825 and 830. Leichtweiss-Institute, Technical University Braunschweig.

Grasmeijer, B.T. and van Rijn, L.C. (1999). Transport of fine sands by currents and waves, III: breaking waves over barred profile with ripples. *J. of Waterway, Port, Coastal, and Ocean Eng., ASCE,* 125(2): 71-79.

Hamilton, D.G. and Ebersole, B.A. (2001). Establishing uniform longshore currents in a large-scale sediment transport facility. *Coastal Engineering,* 42: 199-218.

Herbers, T.H.C., Elgar, S., Guza, R.T. and O'Reilly, W.C. (2006). Surface gravity waves and nearshore circulation. *DUCK94 Experiment Data Server: SPUV Pressure Sensor Wave Height Data,* Available online at: http://dksrv.usace.army.mi/jg/dk94dir.

Hurue, M. (1990). *Two-Dimensional Distribution of Undertow due to Irregular Waves,* B.Eng. Thesis. Dept. of Civil Eng., Yokohama National University, Japan (in Japanese).

Johnson, H.K. (2006). Wave modelling in the vicinity of submerged breakwaters. *Coastal Engineering,* 53: 39-48.

Kraus, N.C., Gingerich, K.J. and Rosati, J.D. (1989). *DUCK85 Surf Zone Sand Transport Experiment,* Technical Report CERC-89-5. US Army Corps of Engineers, Waterways Experiment Station.

Kraus, N.C. and Smith, J.M. (1994). *SUPERTANK Laboratory Data Collection Project,* Technical Report CERC-94-3. US Army Corps of Engineers, Waterways Experiment Station, Vol. 1-2.

Miche, R. (1951). Le pouvoir reflechissant des ouvrages maritime exposes a l'action de la houle. *Annales Ponts et Chaussees,* 121 Annee, pp. 285-319.

Nairn, R.B. (1990). *Prediction of Cross-Shore Sediment Transport and Beach Profile Evolution,* Ph.D. thesis, Dept. of Civil Eng., Imperial College, London.

Oliveira, F.S.B.F. (2007). Numerical modeling of deformation of multi-directional random wave over a varying topography. *Ocean Engineering,* 34: 337-342.

Rattanapitikon, W., Karunchintadit, R. and Shibayama, T. (2003). Irregular wave height transformation using representative wave approach. *Coastal Engineering Journal, JSCE,* 45: 489-510.

Roelvink, J.A. and Reniers A.J.H.M. (1995). *LIP 11D Delta Flume Experiments: A Data Set for Profile Model Validation,* Report No. H 2130. Delft Hydraulics.

Ruessink, B.G., Walstra, D.J.R. and Southgate, H.N. (2003). Calibration and verification of a parametric wave model on barred beaches. *Coastal Engineering,* 48: 139-149.

Smith, J.M. and Kraus, N.C. (1990). *Laboratory Study on Macro-Features of Wave Breaking Over Bars and Artificial Reefs,* Technical Report CERC-90-12. US Army Corps of Engineers, Waterways Experiment Station.

Southgate, H.N. and Nairn, R.B. (1993). Deterministic profile modelling of nearshore processes. Part 1. Waves and currents, *Coastal Engineering,* 19: 27-56.

Sultan, N. (1995). *Irregular Wave Kinematics in the Surf Zone,* Ph.D. Dissertation. Texas A&M University, College Station, Texas, USA.

Thornton, E.B. and Guza, R.T. (1983). Transformation of wave height distribution. *J. Geophysical Research*, 88(C10): 5925-5938.

Thornton, E.B. and Guza, R.T. (1986). Surf zone longshore currents and random waves: field data and model. *J. of Physical Oceanography,* 16: 1165-1178.

Ting, F.C.K. (2001). Laboratory study of wave and turbulence velocity in broad-banded irregular wave surf zone. *Coastal Engineering,* 43: 183-208.